Received: 23 June 2022 | Revised: 13 September 2022 | Accepted: 15 September 2022

DOI: 10.1111/mec.16703

ORIGINAL ARTICLE

MOLECULAR ECOLOGY WILEY

The dynamic response to hypo-osmotic stress reveals distinct stages of freshwater acclimation by a euryhaline diatom

Kala M. Downey | Kathryn J. Judy | Eveline Pinseel | Andrew J. Alverson | Jeffrey A. Lewis

Department of Biological Sciences, University of Arkansas, Fayetteville, Arkansas, USA

Correspondence
Jeffrey A. Lewis and Andrew J. Alverson, Department of Biological Sciences, University of Arkansas, Fayetteville, AR 72701 USA.
Email: lewisja@uark.edu and aja@uark.edu

Funding information
Arkansas Biosciences Institute; Belgian American Educational Foundation; National Science Foundation, Grant/Award Number: DEB-1651087 and MCB-1941824; Simons Foundation, Grant/Award Number: 403249 and 725407; Fulbright Belgium

Handling Editor: Mitchell Cruzan

Abstract

The salinity gradient separating marine and freshwater environments is a major ecological divide, and the mechanisms by which most organisms adapt to new salinity environments are poorly understood. Diatoms are a lineage of ancestrally marine microalgae that have repeatedly colonized and diversified in freshwaters. *Cyclotella cryptica* is a euryhaline diatom found in salinities ranging from fully freshwater to fully marine, thus providing a powerful system for understanding the genomic mechanisms for mitigating and acclimating to low salinity. To understand how diatoms mitigate acute hypo-osmotic stress, we abruptly shifted *C. cryptica* from seawater to freshwater and performed transcriptional profiling during the first 10 h. Freshwater shock dramatically remodelled the transcriptome, with ~50% of the genome differentially expressed in at least one time point. The peak response occurred within 1 h, with strong repression of genes involved in cell growth and osmolyte production, and strong induction of specific stress defence genes. Transcripts largely returned to baseline levels within 4–10 h, with growth resuming shortly thereafter, suggesting that gene expression dynamics may be useful for predicting acclimation. Moreover, comparison to a transcriptomics study of *C. cryptica* following months-long acclimation to freshwater revealed little overlap between the genes and processes differentially expressed in cells exposed to acute stress versus fully acclimated conditions. Altogether, this study highlights the power of time-resolved transcriptomics to reveal fundamental insights into how cells dynamically respond to an acute environmental shift and provides new insights into how diatoms mitigate natural salinity fluctuations and have successfully diversified across freshwater habitats worldwide.

KEYWORDS
Cyclotella cryptica, marine microbiology, salinity stress, stress acclimation, transcriptional dynamics

1 | INTRODUCTION

All organisms experience environmental fluctuations and so have evolved robust responses to abiotic stressors such as suboptimal temperatures, nutrients, and salinities. Salinity stress is particularly important for aquatic organisms ranging from microbes to algae and fish, where the majority live exclusively in marine or freshwater environments. However, some "euryhaline" species have evolved to tolerate a wide range of salt concentrations, allowing them to grow in environments with fluctuating salinities such as lagoons, estuaries, and coastal intertidal zones. The salinity in these habitats can vary in time from fresh to fully marine levels, and salinity shifts in these

systems can occur gradually or within minutes to hours depending on rainfall, river discharge, or tidal action (Balzano et al., 2015). Climate change is expected to increase the frequency and magnitude of these fluctuations. For example, the prevalence of large storms that inundate coastal habitats with freshwater from both precipitation and increased river flow is expected to increase in the future (Pörtner et al., 2019; Shu et al., 2018), and many marine and brackish environments will probably experience "freshening" due to melting ice caps and altered precipitation patterns (Lee et al., 2022).

The effects of fluctuating salinities have been studied in model euryhaline fish, plant, and invertebrate species (Evans, 2009; Negrão et al., 2017; Zanotto & Wheatly, 2006), with the logic that these organisms have evolved osmoregulatory strategies to deal with both transient fluctuations and prolonged exposure to new salinities. Some conserved mechanisms for dealing with salinity change have been observed. For example, hypo-osmotic stress results in water influx that increases intracellular turgor pressure, which risks rupturing the plasma membrane (Kirst, 1990; Theseira et al., 2020; Van Bergeijk et al., 2003). One conserved cellular response in model organisms from the plant, fungal, and animal kingdoms, is to modulate ion and osmolyte levels to maintain osmotic balance (Evans, 2009). Additionally, cells can regulate the activity of water transporters (aquaporins) to rapidly adjust the permeability of membranes to water (Tanghe et al., 2006; Tyerman et al., 2002, 2021). Aquatic animals such as fish can additionally tune the expression and activity of ion transporters in osmoregulatory organs, while also adjusting drinking and urination rates to further maintain osmotic balance (Evans, 2009; Kültz et al., 2015).

Although aquatic microalgae lack behavioural and organ-level mechanisms for responding to salinity stress, numerous euryhaline species nevertheless thrive across a wide range of salinities, highlighting the presence of robust cellular mechanisms for mitigating the effects of salinity changes. As such, these species present an excellent opportunity to investigate the molecular mechanisms underlying these responses, which is important for understanding how ecologically important species will respond to increasingly dynamic salinity environments.

Diatoms, a diverse group of globally distributed microalgae that are abundant in habitats across the entire marine to freshwater salinity gradient, and across evolutionary timescales, transitions between marine and fresh waters have been an important source of species diversification (Nakov et al., 2018). *Cyclotella cryptica* is one of many euryhaline diatom species that occurs naturally in freshwater, brackish, and marine ecosystems (Cavalcante et al., 2013; Houk et al., 2010), and as part of an ancestrally freshwater clade (Roberts et al., 2022), is an important model for understanding the effects of salinity on diatom physiology. For example, salinity is known to impact the morphology of the siliceous cell wall of *C. cryptica*, including alterations to its thickness and ornamentation (Conley et al., 1989; Schultz, 1971). Acute salinity shifts can also induce gametogenesis in *C. cryptica* (Schultz & Trainor, 1970) and other diatoms (Godhe et al., 2014). Like other multi- and unicellular organisms, diatoms respond to salinity stress by modulating internal osmolyte concentrations, which is accomplished through transport of inorganic ions such as sodium or potassium (Hohmann, 2002; Krell et al., 2008; Schultz & McCormick, 2012), or by degrading organic osmolytes such as dimethylsulfoniopropionate (DMSP) (Lyon et al., 2011, 2016), glycine betaine (Dickson & Kirst, 1987; Kageyama et al., 2018), or proline (Hayat et al., 2012; Krell et al., 2007; Liu & Hellebust, 1974). In the initial minutes and hours following hypo-osmotic stress, *C. cryptica* reduces the concentration of osmolyte-functioning amino acids by incorporating them into proteins (Liu & Hellebust, 1974, 1976). However, longer-term transcriptional profiling experiments suggest that reduced proline levels do not appear to play an important role in long-term acclimation, where instead cells maintain reduced levels of glycine betaine, DMSP, and taurine (Nakov et al., 2020). Discrepancies over which processes are important over different time scales has led to substantial debate, not only in diatoms, but in other organisms as well (Borowitzka, 2018; Davies, 2016; Schulte, 2014). Which cellular processes organisms rely upon to withstand short-term stress versus long-term acclimation remains an important open question. To address these gaps in our understanding of the transcriptional response to hypo-osmotic stress, we exposed a brackish strain of *C. cryptica* to freshwater and used RNA sequencing (RNA-seq) to characterize changes in gene expression in the minutes to hours following a freshwater shock. Comparisons to expression-level changes in fully acclimated cells of *C. cryptica* revealed important differences between short- and long-term responses to hyposalinity conditions. Altogether, the results from this study highlight the power of time-resolved transcriptomics during an acute and dynamic environmental response, which we leveraged to provide new insights into how diatoms mitigate natural salinity fluctuations to eventually colonize and diversify across freshwater habitats worldwide.

2 | MATERIALS AND METHODS

2.1 | Culture conditions

Cyclotella cryptica strain CCMP332 was obtained from the National Center for Marine Algae and Microbiota and maintained in artificial sea water at 24 parts per thousand salinity (ASW 24) (Nakov et al., 2020), typical of the brackish salinity of West Tisbury Great Pond in Martha's Vineyard, MA, USA, where the strain was originally collected (Reimann et al., 1963). To obtain sufficient biomass for subsequent experiments, cells were grown for 7 days in a 500 ml Erlenmeyer flask, placed in a Percival incubator at 15°C and 22 μmol photons m^{-2} s^{-1} irradiance under a 16:8 h light:dark cycle. Cells were homogenized by agitating the flask, and 3 × 2-ml aliquots of cells were used to inoculate 3 × 1 L Erlenmeyer flasks containing 500 ml of ASW 24. Growth was monitored by counting cells with a Benchtop B3 Series FlowCAM cytometer (Fluid Imaging Technologies).

To perform transcriptional profiling, triplicate cultures of cells were grown exponentially in ASW 24 and then immediately

exposed to freshwater conditions (ASW 0), mimicking a dispersal event or rapid environmental fluctuation. To do this, we harvested 2.4×10^7 cells from each 1 L flask, centrifuged the cells at 800 rcf for 3 min at 4°C, decanted the supernatant, and resuspended the cells in 16 ml of ASW 0 to a final concentration of 1.5×10^6 cells/ml. Then, 2 ml aliquots of the resuspended cells were then immediately transferred into eight tubes containing 38 ml of ASW 0, and the cells were incubated at 15°C and 20 µmol photons m^{-2} s^{-1} irradiance with gentle agitation using a Boekel Scientific adjustable speed wave rocker. Cells were collected for transcriptional profiling at eight different time points following inoculation in ASW 0: 0 min, 15 min, 30 min, 1 h, 2 h, 4 h, 8 h, and 10 h. In addition to the 0 min control sample (collected immediately following inoculation in ASW 0), we also collected an untreated control that was collected directly from ASW 24. Cells were harvested by centrifugation at 400 rcf for 3 min at 4°C, flash-frozen in liquid nitrogen, and stored at −80°C until processed.

Cellular growth in ASW 24 and 0 (freshwater) was independently measured at each of the time points used for transcriptional profiling, as well as at 12 h, 24 h, and 7 days. Cells were handled identically as described above for time point collections, after which we transferred a 2-ml aliquot of concentrated cells to a 12-well plate. We treated the concentrated cells with 0.1% Lugol's iodine solution as a fixative, and then counted cells with a Benchtop B3 Series FlowCAM cytometer (Fluid Imaging Technologies).

2.2 | RNA extraction and library preparation

To reduce potential batch effects, numbered samples were randomized using the "sample" function in R version 4.05 prior to RNA extraction and library construction. RNA was extracted with an RNeasy Plant Mini Kit (Qiagen) according to the manufacturer's instructions and quantified with a Qubit 2.0 Fluorometer (Invitrogen). RNA quality was assessed using an Agilent Technologies 2200 TapeStation (Agilent Technologies). RNA concentrations and RNA integrity number (RIN) values are available in Table S1. We constructed dual-indexed RNA libraries with the KAPA mRNA HyperPrep kit (KAPA Biosystems) using half reaction volumes. A detailed protocol can be found on protocols.io: https://doi.org/10.17504/protocols.io.uueewte. Libraries were synthesized using at least 150 ng total RNA, fragmentation time was optimized to generate an average fragment length of 300–400 nt, and libraries were amplified with 10 PCR cycles. Libraries were barcoded using KAPA version 3 dual indices, multiplexed, and sequenced on a single lane of an Illumina HiSeq 4000 (2 × 100 bp paired-end reads) at the University of Chicago Genomics Facility. Additional details are available in Table S1.

2.3 | RNA sequencing analysis

Quality of the raw reads was examined using FASTQC version 0.11.5 (Andrews, 2010). Low-quality reads were removed and adapter sequences trimmed using KTRIM version 1.1.0 (Sun, 2020) with the following settings "-t 15 -p 33 -q 20 -s 36 -m 0.5". Reads were mapped to the reference genome of *C. cryptica* V2 (Roberts et al., 2020) using STAR version 2.7.3a with settings "--alignIntronMin 1 --alignIntronMax 22618" to account for the size distribution of annotated introns (Dobin & Gingeras, 2015). Mapping statistics are available in Table S1. Gene-level counts were quantified from uniquely mapped reads with HTSEQ version 0.11.3 in union mode (Anders et al., 2014) (Table S2).

Trimmed mean of *M*-values (TMM) normalization and differential expression analysis were conducted using the BIOCONDUCTOR package EDGER version 3.30.3 (Robinson et al., 2010). Only genes with at least one read count per million (CPM) in at least three samples were included in the analysis. Global similarity of gene expression patterns at each time point was assessed with metric multidimensional scaling (MDS) of logCPM values for the top 500 genes with largest standard deviations across samples (time points and replicates), using LIMMA's plotMDS function (Ritchie et al., 2015). Both control samples (untreated ASW 24 and 0 min ASW 0 treatment) clustered tightly in the MDS plot, so we used the 0 min ASW 0 treatment, which was handled identically to the stress time point samples, as the common control sample to which stress time points were compared. Differential expression was performed in EDGER using the quasi-likelihood (QL) model (glmQLFit) with a group-model design that included each replicate time point combination and a Benjamini–Hochberg false discovery rate (FDR)-adjusted *p*-value cutoff of 5% (Lund et al., 2012). Each time point was compared to the 0 min ASW 0 control. To take into account testing of multiple hypotheses for each gene across each comparison (i.e., significant differential expression across multiple time points), we used STAGER version 1.14.0, which allowed us to control the gene-level FDR across all contrasts with a 5% cutoff (Heller et al., 2009; Van den Berge et al., 2017).

We compared previously published RNA-seq data from *C. cryptica* CCMP332 after long-term acclimation (120 days) to ASW 0 (Nakov et al., 2020). However, rather than having independent replicates of the same strain, the unit of replication used by Nakov et al. (2020) included four different strains of *C. cryptica* that were all sampled once. Consequently, the Nakov et al. (2020) data set included only one sample for *C. cryptica* strain CCMP332. To accommodate this limitation, we followed recommendations by Robinson et al. (2010) for unreplicated data and used the EDGER exactTest function with an assigned dispersion of 0.16 to identify genes with differential expression when contrasting an unstressed control in ASW 24 versus the long-term (120 days) acclimated growth in ASW 0 measured by Nakov et al. (2020). To further compensate for the lack of replication, we restricted our analyses to genes with ≥1 $\log_2$-fold change. The outputs from all differential expression analyses can be found in Table S3.

Hierarchical clustering was performed with CLUSTER version 3.0 (Eisen et al., 1998) using uncentered Pearson's correlation as the similarity metric and centroid linkage. Gene ontology (GO) enrichment analyses were conducted using the elim algorithm and Fisher's exact test implemented in TOPGO version 2.36.0 (Alexa &

Rahnenfuhrer, 2022), with Bonferroni-corrected *p*-values ≤ .05 considered significant.

Functional gene annotations were based primarily on the published annotation of the reference genome (Roberts et al., 2020) but were augmented in some cases with NCBI-BLASTP (Altschul et al., 1990) searches against the Swissprot and Uniprot databases with an *e*-value cutoff 1e-6. KEGG pathway annotations were obtained from the KofamKOALA web server on 2020-09-17 (Aramaki et al., 2020). Related GO terms were condensed using the online server REVIGO (Supek et al., 2011) based on a 0.5 similarity threshold using the SIMREL algorithm. We detected orthologues of *C. cryptica* genes in other diatom genomes using ORTHOFINDER version 2.2.6. (Emms & Kelly, 2015) with the following settings: "-a 24 -t 24 -S diamond -f genomes_for_orthofinder -og". Orthologues of *Seminavis robusta* cell cycle marker genes were obtained from Bilcke et al. (2021), and orthologues of *C. nana* (formerly *Thalassiosira pseudonana*) diel-regulated genes were obtained from Goldman et al. (2019). All code used in this manuscript are provided as Markdown files in Appendices S1 and S2.

3 | RESULTS

3.1 | Hypo-osmotic stress causes transcriptional remodelling in *C. cryptica* that parallels transient growth arrest and acclimation

To understand the physiological and transcriptomic effects of acute hypo-osmotic shock, we transferred *C. cryptica* strain CCMP332 from its native, brackish salinity (ASW 24) into freshwater (ASW 0), mimicking a dispersal event or rapid environmental fluctuation. Following exposure to freshwater, we measured cell division in the first hours and up to 7 days, and used RNA-seq to characterize patterns of gene expression across eight time points within the first 10 h.

Both the freshwater stressed and control ASW 24 samples experienced an initial loss in cell density, which was greater in the freshwater treatment than the control (Figure 1). We have observed similar decreases in experiments and routine transfers, though why it occurs is unclear. Nonetheless, the untreated cultures recovered from this loss within 60 min, while the freshwater cultures experienced a longer lag phase, consistent with growth arrest caused by salinity shock in the 4 h immediately following freshwater exposure (Figure 1). Transient arrest of the cell cycle during stress is common in eukaryotes (Nitta et al., 1997; Seaton & Krishnan, 2016; Skirycz et al., 2011; West et al., 2004), and is probably important for redirecting cellular resources away from growth and towards induction of stress defence genes (Ho et al., 2018). Consistent with this hypothesis, maximal changes in gene expression also peaked during this period of arrested growth (Figure 1). Moreover, genes that would be expected to be expressed during cell growth (e.g., S-phase specific and cell wall related genes) were largely repressed during the early time points before recovering (Figure S1), providing transcriptional evidence for cell cycle arrest. Once growth resumed, *C. cryptica* showed a reduced growth rate in freshwater over the course of 7 days compared to the ASW 24 brackish water control (doubling time of 147 h in ASW 0 vs. 86 h in ASW 24, Figure 1). This is consistent with our previous observation of a reduced growth rate for long-term (120-day) freshwater acclimated *C. cryptica* CCMP332 compared to growth in the brackish (ASW 24) control (Nakov et al., 2020).

Transcriptional profiling revealed substantial remodelling of global gene expression during acute hypo-osmotic stress. Of the 21,250 predicted genes in the *C. cryptica* genome, 12,939 (61%) of them were expressed under the conditions of the experiment (defined as counts per million > 1 in at least 3 samples). Among these expressed genes, 10,566 (82%) were differentially expressed in at least one time point compared to the unstressed control (FDR < 0.05). This corresponds to roughly half of all genes in the genome, highlighting the profound effects of hypo-osmotic stress on the ability of *C. cryptica* to maintain homeostasis. A large fraction (31%) of differentially expressed genes were induced or repressed less than 1.5-fold, which we interpret as hypo-osmotic stress causing subtle, yet reproducible, downstream effects on many aspects of *C. cryptica* physiology. For example, at 60 min there was slight upregulation of genes encoding proteins involved in redox functions and regulation of potassium channels, and a slight downregulation of many genes

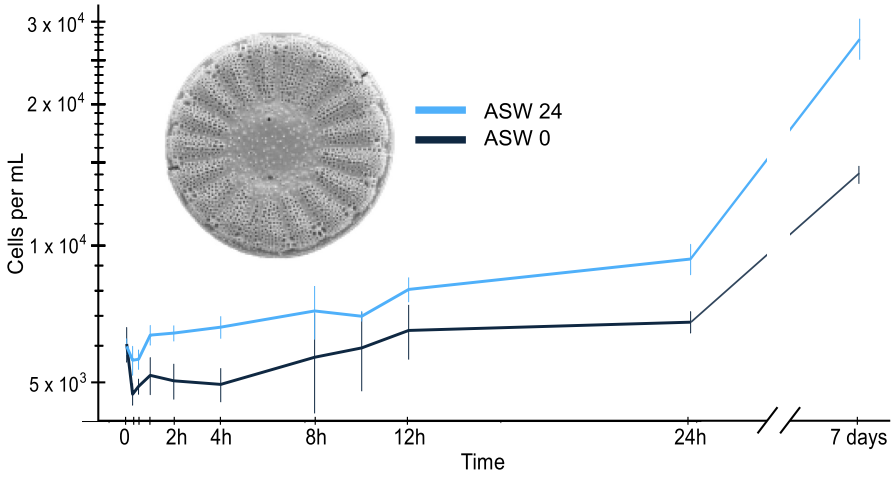

FIGURE 1 Hypo-osmotic shock causes transient growth arrest in *Cyclotella cryptica* followed by acclimation to a reduced growth rate. Cell counts were obtained for *C. cryptica* transferred to freshwater (ASW 0) compared to its native brackish water control (ASW 24) over a 7-day period. Error bars denote the standard deviation of biological triplicates. The inset image is a scanning electron micrograph of *C. cryptica* strain CCMP332 (cell diameter ≈ 10 μm). Raw count data are available in Table S4. [Colour figure can be viewed at wileyonlinelibrary.com]

associated with macromolecule localization and metal ion transport (Table S5).

With the rationale that the genes most critical to the hypo-osmotic response should have consistent patterns of differential expression across time, we narrowed our focus to genes with significant differential expression in the same direction for at least two consecutive time points. A total of 4298 genes met this criterion and were included in downstream analyses. The largest numbers of differentially expressed genes, and the largest magnitude of expression changes, occurred at the 30 and 60 min time points (Figure 3a), indicating that the peak of the transcriptional response occurred within this time frame. An MDS plot comparing the overall similarity of expression profiles at each time point showed that the 30 and 60 min samples were the least similar to the control (Figure 2). Genes encompassing the peak response gradually returned to near baseline levels by 4–10 h (Figures 2 and 3b). Notably, that 4–10 h time period coincided with the resumption of growth (Figures 2 and 3b), suggesting that the short-term acute transcriptional response to hyposaline stress potentiates growth acclimation (see Section 4).

3.2 | Key differences in the genes and processes that comprise the "peak" and "late" phases of the acute hypo-osmotic stress response

Next, we sought to understand the major biological processes that were differentially regulated in response to hyposalinity stress. The 60 min time point had the largest number of genes (1480) with the greatest magnitude of expression change, suggesting that this time point best captured the peak of the response. These peak response genes largely returned to their prestress levels of expression by 8 h (Figure 4a). Genes significantly induced at least 2-fold at 60 min were enriched for photosynthetic processes, indicators of oxidative stress, and transcriptional regulation (Figure 4c, Table S7). In contrast, genes significantly repressed at least 2-fold at 60 min were enriched for ribosome biogenesis, transcriptional regulation, translational initiation, protein modification and localization, and ATP metabolism (Figure 4c, Table S7). Repression of genes related to protein synthesis and growth is common in eukaryotic stress responses (Gasch et al., 2000; Mayer et al., 2005) and is probably important for redirecting translational capacity towards induced stress-defence transcripts (Ho et al., 2018; Lee et al., 2011).

We were interested in understanding whether late-responding genes had different characteristics compared to peak-response genes. In contrast to the 1480 genes with maximal expression changes at 60 min, only 200 genes experienced their maximal expression change at the 10-h mark (Figure 4b). There was relatively little shared functional enrichment between genes with maximal expression at 60 min versus 10 h, with only "ribosome biogenesis" and "iron ion binding" shared between the two (Figure 4d). This low level of functional overlap was driven by a majority (~80%) of the genes with maximal expression at 60 min returning to nearly prestress expression levels by 10 h (Figure 4a). Intriguingly, genes with maximal expression changes at 10 h had, on average, opposite expression patterns at 60 min (Figure 4a,b). The genes upregulated at 10 h were functionally enriched for ribosome biogenesis, carbon fixation, and general regulation of metabolism—with ribosome biogenesis being notably repressed at 60 min (Figure 4d, Table S7). Likewise, the genes repressed at 10 h were functionally enriched for peptide transport and oxidative stress. In contrast, oxidative stress defence genes were induced at 60 min. One possible explanation for the discordant direction of gene expression changes between the 60 min and 10 h time points is that a subset of genes that respond mildly to acute stress are important for the early stages of acclimation. For example, the timing of derepression of ribosome biogenesis genes, which are required for cell growth, just precedes growth resumption.

3.3 | Groups of functionally related genes show distinct expression subdynamics during hypo-osmotic stress

While the overall peak of the hypo-osmotic stress response occurred approximately 60 min after introduction into freshwater, hierarchical clustering revealed groups of genes with distinct subdynamics that deviated from the behaviour of peak response genes. We collapsed the expression dendrogram into 10 clusters based on their distinct expression profiles (Figure 3b,c). Notably, the expression patterns of five of these clusters (2, 4, 5, 6, and 8) showed short-term changes across the early time points followed by acclimated gene expression patterns (i.e., a return to near baseline), that we hypothesize are related to the short-term growth arrest that occurred during the first 4 h of hypo-osmotic shock (Figure 1). We also found that distinct clusters with similar expression patterns often shared functional enrichments (Figure 3c,d). For example, clusters enriched for "ion transporter activity" and "oxidoreductase activity" (Figure 3c,d; Clusters 2, 4, and 6) were generally induced between 30 and 60 min then downregulated from 2 h onward. Conversely, clusters enriched for genes involved in transcription, translation, and ribosome biogenesis (Figure 3c,d; Clusters 1 and 5) were repressed between 15 and 60 min, followed either by a return to baseline expression (Cluster 5) or upregulation (Cluster 1) between 2 and 10 h. Cluster 8, enriched for genes involved in energy production (Krebs cycle and ATP synthesis-coupled proton transport), showed similar dynamics to the "translation-related" Clusters 1 and 5, suggesting that these processes might be coordinately regulated during hypo-osmotic stress.

Although the majority of genes fell into clusters where expression changes peaked within 30–60 min, four clusters had unique expression patterns. Cluster 3 showed constant upregulation and was enriched for both positive and negative regulation of transcription, and defence against oxidative stress. In contrast, Cluster 7 showed continuous downregulation at all time points and was enriched for processes related to macromolecule trafficking and negative regulation of cell division and DNA replication. Finally, clusters with the smallest gene membership (Clusters 9 and 10) showed either delayed

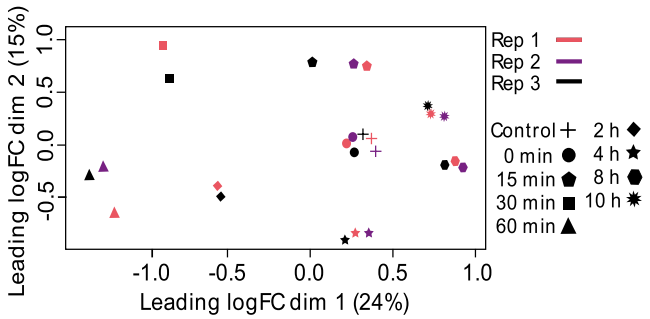

FIGURE 2 Multidimensional scaling (MDS) plot of the acute response to hypo-osmotic stress. MDS analysis was performed on the logCPM values for the top 500 genes with the largest standard deviations across samples. [Colour figure can be viewed at wileyonlinelibrary.com]

repression (Cluster 9) or delayed induction (Cluster 10). Annotated genes in Cluster 9 were enriched for genes associated with chitin metabolism, while the few known genes in Cluster 10 were enriched for photosynthesis-related processes and ribonuclease III activity. Clusters 9 and 10 also had a high proportion of uncharacterized genes (25% and 50%, respectively), so the biological implications of these late responding clusters are not completely clear.

3.4 | Stress defence genes induced by hypo-osmotic stress

To understand how *C. cryptica* maintains homeostasis during acute hypo-osmotic shock, we analysed the expression of genes known to play a role in stress defence in other species. Hypo-osmotic shock initially causes an influx of water and efflux of ions and other osmolytes, so we examined how genes that encode channels and transporters responded throughout the time course. None of the genes encoding aquaporin water channels were significantly differentially expressed at two consecutive time points, though one was strongly induced at 30 min (Figure S2). A total of 15 K^+ channels and pumps were upregulated at intermittent periods throughout the experiment, as were 17 Na^+ exchangers and pumps. These transporters were primarily grouped into Clusters 2 and 5, which display contrasting expression patterns. This may indicate that the genes required to maintain the ion gradient changed over time. In addition to transmembrane transporters in the cell membrane, two chloroplastic K^+ efflux pumps were upregulated. Hypo-osmotic stress also triggered upregulation of a mechanosensitive anion transporter in the plasma membrane from 30 min to 3 h, potentially due to cell sensing of increased osmotic pressure. Outside of the subset of genes differentially expressed at two consecutive time points, an additional 66 K^+ and Na^+ transporters were differentially expressed at only one time point, with no consistent pattern of when differential expression occurred and with a roughly equal distribution of up- and downregulation.

Cells can respond to increased turgor pressure from hypo-osmotic stress by regulating intracellular osmolyte concentrations. Diatoms achieve osmotic balance by modulating concentrations of low-molecular weight osmolytes including DMSP, taurine, glycine-betaine, and proline (Boyd & Gradmann, 2002; Tevatia et al., 2015). Several essential steps in proline biosynthesis were downregulated (Figure S2), suggesting that stressed cells decreased the intracellular concentration of this key osmolyte. For taurine, two genes involved in its degradation were repressed at various time points, suggesting that cytosolic taurine levels may actually be increasing during acute hypo-osmotic stress in *C. cryptica* (Figure S2). There was no transcriptional evidence that cells adjusted the concentrations of other osmolytes within the 10 h following freshwater exposure. For DMSP and glycine-betaine biosynthesis, neither of the two methyltransferases critical for their biosynthesis were differentially expressed (Table S3).

In addition to genes directly involved in maintaining osmotic balance, other classes of stress defence genes were also differentially expressed during the time course. This includes a number of genes involved in scavenging reactive oxygen species (ROS). Out of 11 probable thioredoxins, two were upregulated at different time points (Figure 3c; Clusters 1 and 2, Figure S3), while one was downregulated for the duration of the experiment. We also identified five differentially expressed chloroplastic peroxiredoxins, with four upregulated at different time points and one strongly downregulated at all time points. Several ROS scavengers were upregulated around the peak period of the hypo-osmotic stress response (30–60 min): two superoxide dismutases, one catalase, and one L-ascorbate peroxidase (Figure S3). A total of 15 of 28 putative heat shock protein (HSP) chaperones were differentially expressed, with the majority of them (12/15) downregulated at the peak period of the stress response, and becoming slightly upregulated or returning to baseline levels by 4 h. The remaining three HSP chaperones showed the opposite pattern, being upregulated from 30–60 min and returning to baseline levels or becoming slightly repressed by 4 h (Figure S4).

3.5 | Expression dynamics of metabolic pathways during hyposaline stress

In addition to "classic" stress defence genes, hypo-osmotic stress resulted in substantial transcriptional remodelling of numerous other metabolic genes in *C. cryptica*. Below, we summarize effects on several main metabolic pathways.

3.5.1 | Krebs cycle

One of the two copies of the gene that encodes citrate synthase, which catalyses the first step of the Krebs cycle, was slightly upregulated for the duration of the time course (Figure 5, Figure S5). However, the enzymes responsible for catalysing the next steps were either not differentially expressed or were mildly downregulated for the first 2 h followed by recovery to approximately unstressed levels by 4–8 h.

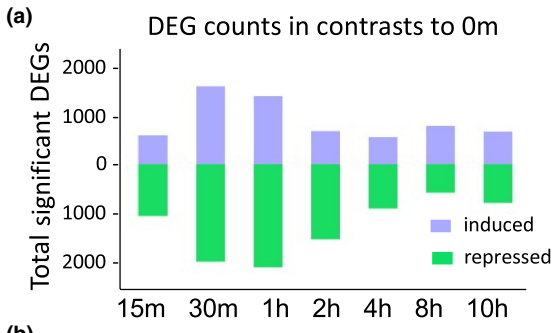

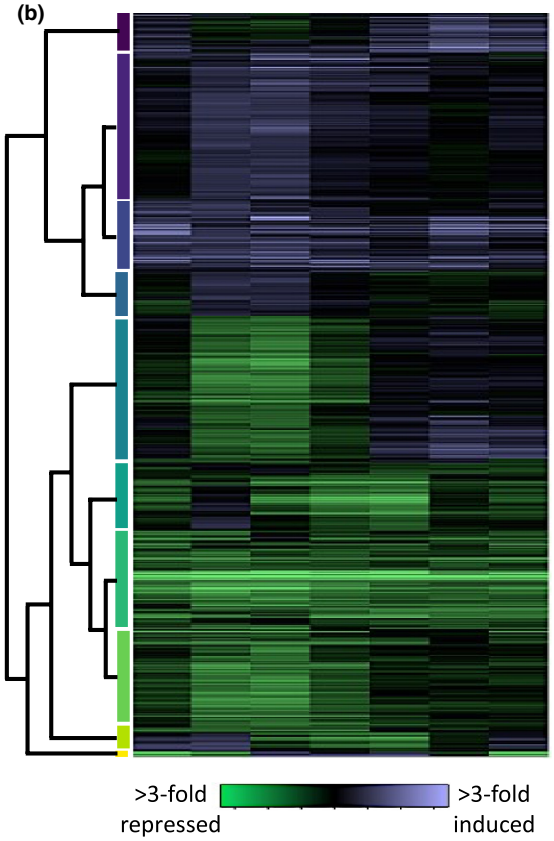

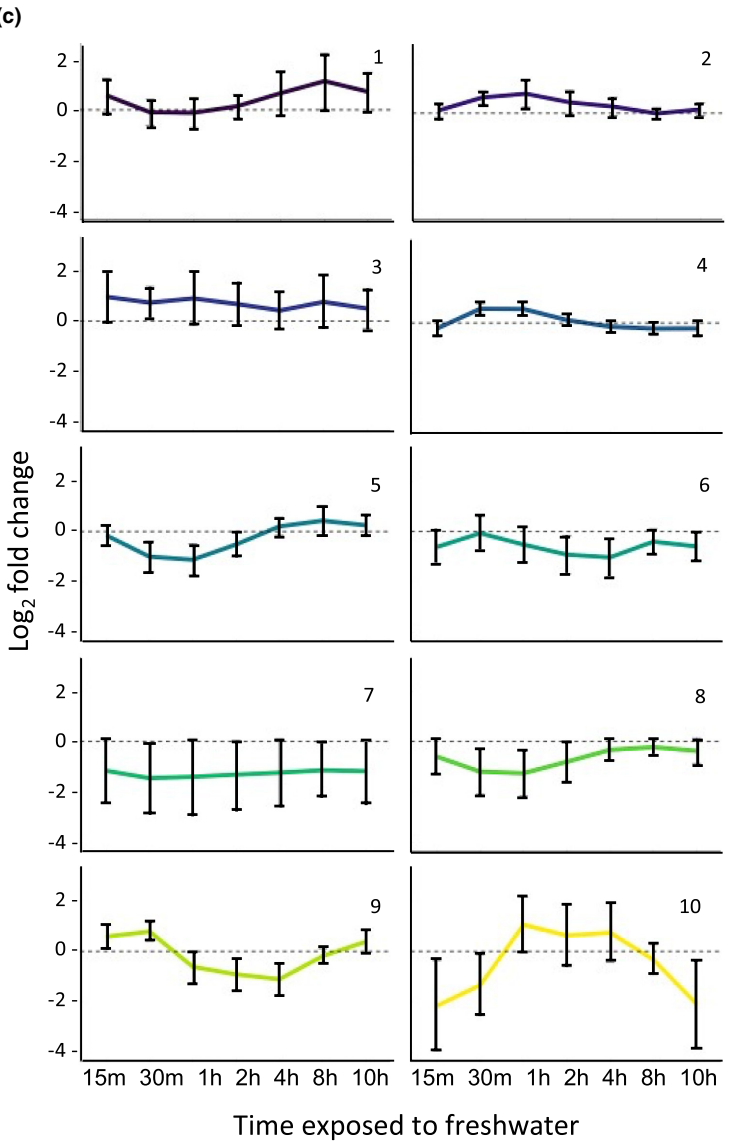

(d)

Cluster	No. genes	Enriched GO terms p < 0.01
1	243	rRNA processing^{BP}, DNA-binding transcription factor activity^{MF}
2	849	Photosynthesis (light harvesting)^{BP}, metal ion transport^{BP}, solute:proton antiporter activity^{MF}, violaxanthin de-epoxidase activity^{MF}, oxidoreductase activity^{MF}
3	410	Transcription regulation^{BP}, sulfur compound synthesis^{BP}, iron ion binding^{MF}
4	252	Cellular amino acid catabolism^{BP}, inward potassium channel activity^{MF}, oxidoreductase activity^{MF}
5	848	Ribosome biogenesis^{BP}, translation initiation^{BP}, GTP binding^{MF}
6	494	Carboxylic acid catabolism^{BP}, oxidoreductase activity^{MF}, cobalamin binding^{MF}, iron ion binding^{MF}
7	465	Macromolecule localization^{BP}, negative regulation of biological processes^{BP}, NADP binding^{MF}, endonuclease activity^{MF}
8	590	Kreb cycle^{BP} , mRNA transport^{BP}, ATP synthesis coupled proton transport^{BP}, RNA binding^{MF}, GTP binding^{MF}
9	108	Carbohydrate metabolism^{BP}, chitin binding^{MF}
10	29	Photosynthesis (light harvesting)^{BP}, ribonuclease III activity^{MF}, ferric iron binding^{MF}

FIGURE 3 Substantial and dynamic remodelling of the *Cyclotella cryptica* transcriptome during hypo-osmotic stress. (a) Total number of significant differentially expressed genes (DEGs) that respond to hypo-osmotic stress at each time point relative to the control. (b) Heat map depicting hierarchical clustering of $\log_2$ fold changes of 4298 genes that were differentially expressed at two or more consecutive time points. Each row represents a gene, and each column represents a time point following exposure to hypo-osmotic stress. Purple indicates induced genes and green indicates repressed genes in response to hypo-osmotic stress, according to the key. (c) Mean $\log_2$ fold changes for 10 clusters (panel b), organized from top to bottom according to the vertical colour key next to the heat-map dendrogram (panel b). Error bars represent the 95% confidence interval for all genes within a cluster. (d) Enriched functional groups for each cluster (Bonferroni-corrected $p < .01$). Superscripts denote biological process (BP) or molecular function (MF) gene ontology (GO) categories. Full GO annotations for each cluster can be found in Table S6. [Colour figure can be viewed at wileyonlinelibrary.com]

3.5.2 | Photosynthesis and carbon fixation

A total of 14 out of 24 genes associated with chlorophyll production, including three magnesium chelatase subunits that initiate chlorophyll biosynthesis (Papenbrock et al., 2000), were upregulated at 30–60 min (Table S9). Additionally, 21 of the 26 genes that encode binding proteins for light-harvesting pigments were upregulated during this time period. Xanthophyll cycle genes coding for zeaxanthin and violaxanthin de-epoxidase were upregulated at 30–60 min and 30 min–4 h, respectively. In contrast, genes associated with light-independent reactions of the Calvin cycle were either downregulated or not differentially expressed during the peak stress response. Most returned to baseline expression levels or became slightly upregulated at 4 h. However, the gene necessary for the two-step conversion of glyceraldehyde-3-phosphate to fructose-6-phosphate, a key intermediate for both glycolysis and chitin biosynthesis, was upregulated during the peak response.

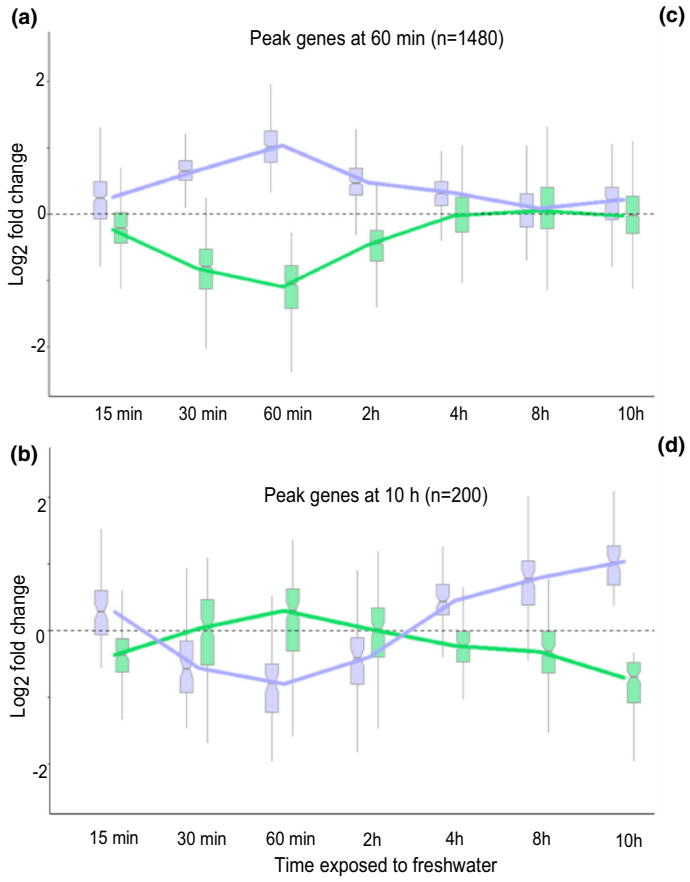

(c)

Molecular Function	GO ID	Down	Up	P-value
DNA-binding transcription factor activity	GO:0003700		97	5.6 e-04
Sequence-specific DNA binding	GO:0043565		128	5.8 e-04
Oxidoreductase activity, affects paired donors	GO:0016705		85	8.5 e-03
Iron ion binding	GO:0005506		91	1.1 e-02
Structural constituent of ribosome	GO:0003735	98		8.6 e-17
RNA binding	GO:0003723	215		1.9 e-05
Aminoacyl-tRNA ligase activity	GO:0004812	41		1.7 e-04
NADP binding	GO:0050661	23		3.1 e-03
GTP binding	GO:0005525	109		3.5 e-03
Biological Processes				
Cyclic nucleotide biosynthetic process	GO:0009190		31	1.5 e-02
Photosynthesis	GO:0015979		60	1.8 e-02
Regulation of transcription, DNA-templated	GO:0006355		203	2.0 e-02
Photosynthesis, light harvesting	GO:0009765		41	3.1 e-02
Glycolytic process	GO:0006906	34		4.8 e-06
rRNA processing	GO:0006906	31		3.2 e-04
Protein folding	GO:0006457	32		1.9 e-03
ATP metabolic process	GO:0046034	47		4.1 e-03
Translational initiation	GO:0006413	18		4.3 e-03

(d)

Molecular Function	GO ID	Down	Up	P-value
Carbohydrate binding	GO:0030246		69	2.5 e-02
Coenzyme binding	GO:0050662	228		3.2 e-02
Vitamin binding	GO:0019842	115		3.2 e-02
Iron ion binding	GO:0005506	91		1.5 e-02
Protein serine/threonine kinase activity	GO:0004674	29		2.3 e-03
Biological Processes				
Regulation of metabolic process	GO:0019222		247	2.3 e-02
Ribosome biogenesis	GO:0042254		51	4.7 e-03
Nitrogen compound transport	GO:0071705	146		1.6 e-02
Peptide transport	GO:0015833	111		2.7 e-02

Key
- ★ Photosynthesis, carbon fixation & glycolysis/gluconeogenesis Oxidative stress
- ● Ribosome biogenesis & transcription regulation
- ■ Translation & protein modification/movement
- – Other

FIGURE 4 Distinct cellular processes are regulated during the peak versus late acute hypo-osmotic response. (a) Box and whisker plots of significantly differentially expressed genes with the highest magnitude of change at 60 min (1480 genes) versus (b) 10 h (200 genes). Boxes represent the median and interquartile ranges, the notches bracketing the median represent the 95% confidence intervals, and the whiskers represent 1.5 times the interquartile range. Genes induced at either 60 min (panel a) or 10 h (panel b) are purple, while repressed genes at the relevant time point comparisons are green. (c, d) Functional enrichments for genes with ≥2-fold induction or repression at 60 min (c), or 10 h (d). Symbols denote major cellular processes associated with each gene ontology (GO) term. Full GO annotations for the 60 min and 10 h time points can be found in Table S7. [Colour figure can be viewed at wileyonlinelibrary.com]

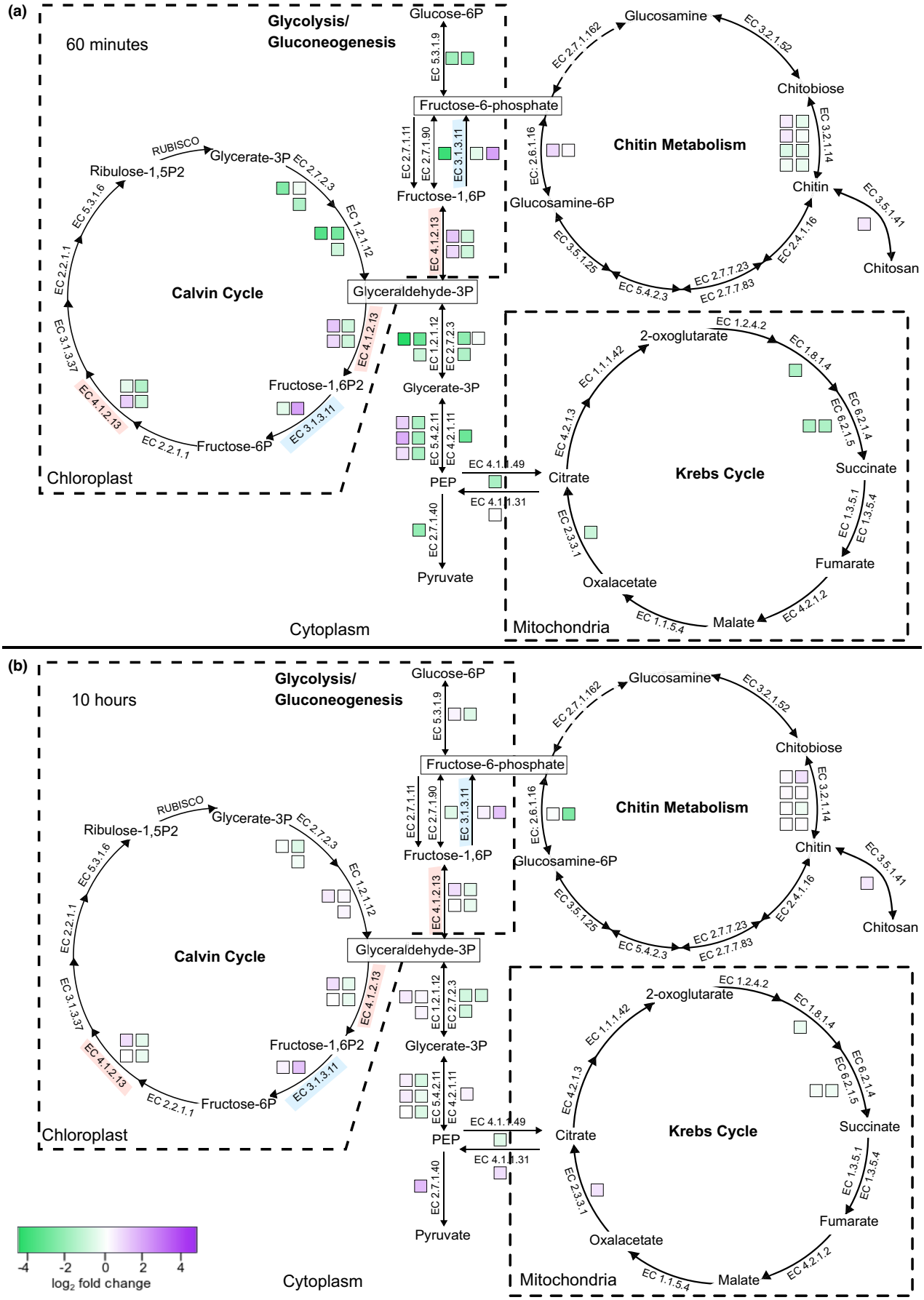

FIGURE 5 Hypo-osmotic stress affects the expression of genes involved in major metabolic pathways. Each coloured square denotes the expression of a single differentially expressed gene at (a) 60 min and (b) 10 h, with purple indicating upregulation and green downregulation according to the key. Enzymatic steps encoded by multiple paralogues are indicated by the presence of multiple boxes (e.g., there are two paralogues for EC 5.3.1.9 responsible for the first step in glycolysis). Dotted lines circumscribe pathways with different organellar compartmentalization, and genes that participate in multiple pathways are separately colour coded (e.g., EC 3.1.3.11 for both the Calvin cycle and gluconeogenesis). [Colour figure can be viewed at wileyonlinelibrary.com]

3.5.3 | Glycolysis and gluconeogenesis

Generally, the genes repressed at 60 min were enriched for glycolysis and gluconeogenesis (Figure 4b). However, there were notable exceptions, including a number of paralogous genes in the pathway showing induction (Figure 5a). To better understand whether flux through glycolysis and gluconeogenesis was being regulated during hypo-osmotic stress, we examined the rate-limiting and irreversible steps of each pathway. For glycolysis, the gene encoding phosphofructokinase-1 was not differentially expressed at either 60 min or 10 h. The gene encoding pyruvate kinase, which is responsible for the last step in glycolysis, was repressed at 60 min, before recovering and ultimately being induced at 10 h. For gluconeogenesis, at 60 min one paralogue encoding the dedicated enzyme fructose 1,6-bisphosphatase was moderately repressed, while the other paralogue was strongly induced. Paralogues encoding fructose-bisphosphate aldolase, the enzyme responsible for the reaction directly preceding that of fructose 1,6-bisphosphatase, showed the same pattern of up- and downregulation. Differential expression of the genes encoding fructose 1,6-bisphosphatase and fructose-bisphosphate aldolase could be due to their shared role in the Calvin cycle, though no other Calvin cycle genes showed similar expression patterns. Instead, we predict that the accumulation of fructose-6-phosphate increases flux towards chitin biosynthesis (see below).

3.5.4 | Chitin biosynthesis

The enrichments of (i) carbohydrate metabolic processes and carbohydrate binding at 60 min, (ii) carbohydrate binding at 10 h (Figure 4b,d), and (iii) carbohydrate metabolism and chitin binding in the "delayed repression" of Cluster 9 (Figure 3d) together highlight chitin biosynthesis as an important part of the response to hypo-osmotic stress. The entire pathway is reversible and initiated by the breakdown of fructose-6-phosphate molecules into glucosamine by glutamine-fructose-6-phosphate transaminase (Figure 5) (Traller et al., 2016). Genes involved in chitin metabolism were largely upregulated at 60 min, as well as the gene responsible for its conversion into the more fibrous chitosan molecule (Figure 5a). Notably, all four paralogues for chitin synthase were strongly upregulated at 30 min (Figure S5). Given these patterns, combined with the predicted accumulation of the key intermediate fructose-6-phosphate, it is likely that chitin biosynthesis is being favoured over degradation. We hypothesize that increased chitin and chitosan production might be important for cell wall remodelling during acute hypo-osmotic stress (see Section 4).

3.5.5 | Diel-responsive genes

Because we compared our stress sample time points to a single control time point, one potential confounder is that some genes may be changing in expression due to the *C. cryptica* diel (or circadian) response. To address whether this was an important confounding variable, we compared our time course data with a transcriptomic data set for (Goldman et al., 2019) that characterized changes in gene expression during peak light versus dark (12 h light:dark cycles), where >60% of genes show significant differential expression. We first performed hierarchical clustering on all significantly differentially expressed genes from our acute freshwater response time course (at any time point to be as inclusive as possible), and then appended the diel response of the corresponding *C. nana* orthologues. If the diel response was at least in part driving the stress-induced expression patterns in our experiment, we would expect stress-induced clusters to be enriched for orthologues expressed during light, and stress-repressed clusters to be enriched for orthologues repressed during light (or expressed during the dark). Instead, we found no consistent pattern of different clusters being enriched for light- or dark-expressed genes (Figure S6a). Likewise, we saw no consistent pattern when we performed the reciprocal clustering on significant diel-responsive *C. nana* orthologues with the *C. cryptica* hypo-osmotic response appended (Figure S6b). Although it is possible that some individual diel-responsive genes are being influenced by both the diel response and hypo-osmotic stress in this study, our interpretation is that the hypo-osmotic response dominates the expression patterns. Because environmental shifts can happen at any time, this does raise interesting questions about whether and how the hypo-osmotic response may change if a freshwater shock occurs in low or no light.

3.6 | The gene expression response to acute hypo-osmotic stress is distinct compared to long-term acclimation to low salinity

To understand whether the genes that were important for the acute hyposaline response were also important for long-term acclimation, we reanalysed previously published RNA-seq data for the same brackish *C. cryptica* CCMP332 strain that had been grown in freshwater for 120 days (Nakov et al., 2020). We found strikingly little overlap between the expression patterns for genes differentially expressed during long-term freshwater acclimation compared to the short-term acute stress response from this study (Figure 6). Of the 1220 genes in the post-acclimation data set that were significantly

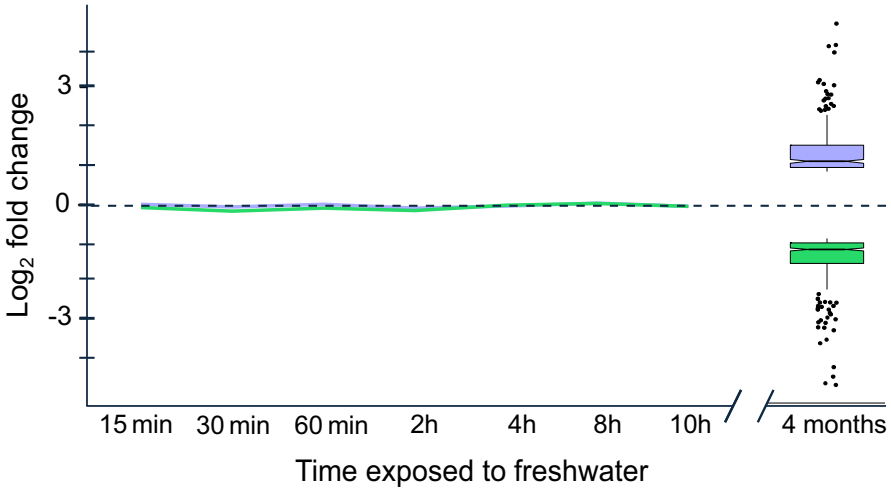

FIGURE 6 The genes differentially expressed during long-term acclimation of *Cyclotella cryptica* to freshwater are distinct from those that respond during acute hypo-osmotic stress. The line graph depicts the average $\log_2$ fold change pattern during our short-term transcriptional profiling for genes that we identified as differentially expressed ≥2-fold following months-long acclimation using data from Nakov et al. (2020). Box and whisker plots show the expression of those genes at 4 months, with boxes representing the median and interquartile ranges, notches bracketing the median representing the 95% confidence intervals, and the whiskers representing 1.5 times the interquartile range. Outliers are shown with dots horizontally jittered for legibility. Gene ontology annotations for differentially expressed genes at 4 months (120 days) can be found in Table S8. [Colour figure can be viewed at wileyonlinelibrary.com]

differentially expressed at least 2-fold, only 259 of them were also differentially expressed at any time point in the short-term stress experiment, representing >2.3-fold under-enrichment ($p < 4.9 \times 10^{-99}$, Fisher's exact test). Although there was significant overlap between genes differentially expressed at the peak 60 min time point and post-acclimated cells, the effect was small (1.03-fold enrichment, $p < 1.1 \times 10^{-6}$). Moreover, the majority of those genes showed opposing directions of differential expression in the acute versus acclimated responses. There was also little overlap between the genes responding to hypo-osmotic stress at 10 h compared to those at 120 days, with just 80 of the 1431 differentially expressed genes at 10 h overlapping with the 1220 differential expressed genes at 120 days. Again, the majority of these overlapping genes at 10 h and 120 days were expressed in opposite. For example, many genes involved in photosynthesis transitioned from being repressed during the acute response to upregulated in fully acclimated cells. Among the few genes with similar expression patterns during the acute and acclimated responses, the majority were genes with unknown function.

Although we observed little overlap in the identity of genes that were differentially expressed during both the acute (0–10 h) and acclimated (120 days) responses, it was still possible that the same functional groups were expressed at both timescales. Enrichment analysis showed no overlap in GO terms for genes involved in the acute versus acclimated responses. In acclimated cells at 120 days, phosphorelay signal transduction was generally repressed, including several strongly repressed genes involved in histidine kinase pathways. Histidine kinases are used by both prokaryotes and eukaryotes as environmental sensors (Abriata et al., 2017), so downregulating these pathways may be a common characteristic of acclimated cells. In contrast, genes involved in DNA replication, DNA methylation, and mRNA splicing were all upregulated in acclimated cells, which may reflect post-acclimation differences in regulation of cell division (Table S3). Despite the caveat that enrichment analysis on the long-term acclimation data may be underpowered due to the absence of replicates, the complete lack of overlap combined with the novel enrichments for the long-term data set are striking. To validate that our approach for analysing the single-replicate long-term acclimation data would probably be robust enough to detect overlap in differentially expressed genes had it existed, we performed the same analysis on a single replicate from our 1 h time point. This resulted in 3102 differentially expressed genes for the single time point, of which there was high and significant overlap (2.7-fold enrichment, $p < 2.6 \times 10^{-358}$) with the 3412 differentially expressed genes found in the "standard" triplicate analysis. The high amount of overlap contrasts sharply with the 2.3-fold under-enrichment seen when comparing the same set of differentially expressed acute-response genes to those differentially expressed during long-term acclimation ($p < 4.9 \times 10^{-99}$), suggesting that the lack of overlap between differentially expressed genes during the acute and long-term response is truly biological rather than due to lack of statistical power. Altogether, these results suggest that the genes and processes necessary for the acute hypo-osmotic stress response and long-term acclimation to freshwater are largely distinct.

4 | DISCUSSION

The goal of this study was to understand how a euryhaline diatom responds to the stress of being immediately immersed in freshwater, a treatment that simulates a dispersal event or a rapid environmental fluctuation. The effects on the transcriptome were rapid and

dramatic—more than 21% of the genes in the genome were differentially expressed within 60 min, and more than half of the genes were differentially expressed for at least one time point, substantially more than the 39% observed when a freshwater strain from the diatom genus *Nitzschia* was exposed to high salinity (Cheng et al., 2014). The types of genes most impacted by hypo-osmotic stress provide new insights into how diatoms maintain homeostasis during an abrupt salinity shift, which has implications for understanding how diatoms have repeatedly diversified into freshwaters and, more pressingly, how they will respond to changes in ocean salinity that are predicted to occur in response to climate change (Lee et al., 2022).

During acute hypo-osmotic stress, cells face an influx of water and increased turgor pressure that risks rupturing the cell membrane, as well as an efflux of ions and other osmolytes that play important roles in cellular metabolism. In such situations, water channels (aquaporins) allow for rapid diffusion of water and sometimes other small molecules such as glycerol (Jahn et al., 2004; Matsui et al., 2018; Tyerman et al., 2002). Because aquaporins are known to play an important role in osmoadaptation (Tanghe et al., 2006), we examined genes encoding aquaporins for differential expression. Although none were significantly differentially expressed at two consecutive time points, one was strongly induced at 30 min (Figure S2). This was somewhat counterintuitive, as high aquaporin expression is associated with increased water influx and potential cell lysis during hypo-osmotic stress (Booth & Louis, 1999; Calamita, 2000). However, induction of an aquaporin during hypo-osmotic stress was also identified recently in another diatom species (Pinseel et al., 2022), and aquaporins may have important roles beyond water transport including signal transduction via osmosensing (Tyerman et al., 2002, 2021).

During either hypo or hypersaline conditions, cells work to restore osmotic balance by adjusting ion gradients, including both Na^+ and K^+ levels (Evans, 2009; Hohmann, 2002; Kültz et al., 2015; Zhu, 2001). During our hypo-osmotic time course, we identified two upregulated chloroplastic K^+ efflux pumps, which might help maintain K^+ concentrations in the chloroplast to maintain proper turgor pressure and photosynthetic efficiency (Kunz et al., 2014; Sheng et al., 2014). Increased osmotic pressure within the cell also triggered upregulation of a mechanosensitive anion transporter in the plasma membrane during 30 min to 3 h. However, the most striking change in expression occurred for cell membrane ion transporters. We identified 17 induced Na^+ exchangers and pumps and 15 induced K^+ channels, suggesting the cell exports Na^+ and H^+ ions and imports K^+ to maintain ion homeostasis (Table S3). An additional 66 K^+ or Na^+ transporter genes were differentially expressed at only one time point, which may indicate that genes required to maintain ion homeostasis change throughout the hypo-osmotic response. Maintaining optimal intracellular ion levels while acclimating to acute hypo-osmotic stress is a major cellular challenge, which *C. cryptica* responds to with a finely-tuned response reflected through the complicated regulation of these myriad transporters throughout the time course. Notably, many channels involved in homeostasis during osmotic stress are mechanosensitive (Kirst, 1990; Kung et al., 2010), so the cell was probably tuning not only expression levels, but also post-translational regulation of these transporters to restore internal ion homeostasis following the initial shock.

Examination of genes involved in osmolyte homoeostasis revealed key differences between the acute response to hypo-osmotic stress (this study) versus months-long freshwater acclimation (Nakov et al., 2020). Glycine-betaine, taurine, and DMSP were all identified as important osmolytes for long-term freshwater acclimation in *C. cryptica*, but we found evidence for different patterns of osmolyte modulation during the short-term acute response. For long-term acclimation, levels of taurine were predicted to decrease, but repression of taurine degradation genes in our experiments are consistent with increased taurine levels in the short-term stress response. Additionally, unlike for long-term acclimation to freshwater, we found no evidence for differential expression of genes involved in DMSP and glycine-betaine metabolism, suggesting their levels do not change during the acute response. In contrast to gene expression levels in *C. cryptica* following acclimation, genes involved in proline metabolism were the only ones differentially regulated during acute freshwater stress. The gene encoding the rate-limiting step of proline biosynthesis (delta-1-pyrroline-5-carboxylate synthetase) was strongly repressed at 30–60 min. A similar pattern of repression was also seen for proline iminopeptidase, an enzyme that breaks down proline-containing peptides into the amino acid constituents (Figure S2). Based on previous carbon-labelling experiments (Liu & Hellebust, 1974, 1976), remaining "free" proline is probably being incorporated into proteins during acute hypo-osmotic stress, rather than being excreted. Because proline is thought to be the main diatom osmolyte that changes in abundance during osmotic shock (Kirst, 1990; Krell et al., 2007), it was surprising at the time to find no changes in proline metabolic gene expression during long-term acclimation (Nakov et al., 2020). Our data suggests that a decrease in proline levels is only critical for the acute phase of the response, which sheds important light on this discrepancy in the literature and underscores the importance of considering different timescales for highly dynamic responses. Taken together, our analysis indicates that the osmolytes necessary during acute hypo-osmotic stress are probably different from the ones that are important for long-term acclimation. This could be a common theme, as the freshwater cyanobacterium, *Synechococcus elongatus*, also showed differences in concentrations of osmolytes during acute versus prolonged treatment with seawater (Liang et al., 2020).

The hypo-osmotic stress response of *C. cryptica* shared features of "general" environmental stress responses seen in other eukaryotes (Gasch et al., 2000; Mager & De Kruijff, 1995), including repression of genes involved in cell growth (e.g., ribosome biogenesis and RNA metabolism) and induction of genes canonically involved in stress defence such as ROS scavengers and HSP chaperones. Like other prokaryotic and eukaryotic microbes (Rojas et al., 2017; Sharfstein et al., 2007; Warner, 1999), diatoms halt cell division in the early stages of osmotic shock until ionic and osmotic equilibria are restored. Under such conditions, energy is probably redirected to cellular processes essential for acute stress management, rather

than energetically expensive processes related to cell growth such as ribosome biogenesis (Albert et al., 2019). In yeast, transcriptional repression during stress appears important for redirecting translational capacity towards induced mRNAs, thereby accelerating production of induced proteins (Ho et al., 2018). Repression of ribosomal transcripts parallels transient growth arrest during stress, and the lack of concomitant ribosomal protein repression suggests that the steady-state level of ribosomes per cell remains similar (Ho et al., 2018; Lee et al., 2011). Ribosomal transcript repression has also been hypothesized as a mechanism for maintaining proteostasis while cells respond to the stressful environment through expression of stress-defence genes (Albert et al., 2019). We also observed a similar downregulation of transcripts for metabolic genes including the Krebs cycle, Calvin cycle, and glycolysis. Because transient growth arrest during stress in yeast leads to a poor correlation between mRNA repression and protein repression (Lee et al., 2011; Storey et al., 2020), caution is warranted when interpreting mRNA downregulation in the absence of proteomics.

Acute hypo-osmotic stress resulted in the induction of many oxidative stress response genes, suggesting that hypo-osmotic stress leads to increase ROS levels. In addition to increased induction of genes encoding direct ROS scavengers (i.e., superoxide dismutase, ascorbate peroxidase, and catalase), other oxidative stress response genes were also induced. Many genes that encode light-harvesting pigment-binding proteins were upregulated throughout the time course, and these proteins are known to help mitigate oxidative stress, in addition to their roles in photosynthesis (Latowski et al., 2011). We also observed upregulation of genes that are expected to increase the concentration of xanthophyll pigments in the cell. These pigments not only function as accessory light-harvesting pigments, but also protect the cell from photo-oxidative damage (Latowski et al., 2011). Polyamine biosynthetic genes were also induced, and polyamines are known to protect against oxidative damage of DNA (Ha et al., 1998). While there is precedent for hyper-osmotic and hypo-osmotic stress causing secondary ROS accumulation (Lyon et al., 2016), it is also possible that hypo-osmotic stress in *C. cryptica* triggers a general stress response. In that case, induction of oxidative stress defence genes during hypo-osmotic stress may reflect shared upstream signalling networks and not hypo-osmotic stress causing oxidative stress per se. An open question in diatom stress biology is whether different species possess a common, generalized stress response, or whether individual stressors have their own unique responses. General stress responses are hypothesized to play a role in cross-stress protection in prokaryotic and eukaryotic microbes as well as plants (Berry & Gasch, 2008; McDaniel et al., 2018; Rangel, 2011; Sabehat et al., 1998). Future studies should examine the transcriptomic response of *C. cryptica* under different stress conditions, and whether hypo-osmotic stress cross protects against other stressors such as elevated temperature or light.

Another striking feature of the hypo-osmotic response was the regulation of many genes related to metabolism, and in particular chitin biosynthesis (Figure 5, Table S9). Chitin is a long-chain polysaccharide notable for playing an analogous role to plant cellulose as the major component of fungal cell walls. Chitin is also found in the cell membrane in a number of different eukaryotic lineages, where it supports skeletal and cell wall structures (Durkin et al., 2009). *Cyclotella* species, including *C. cryptica*, produce β-chitin, which is extruded as long crystalin threads from specialized siliceous pores around the margin of the cell (LeDuff & Rorrer, 2019; McLachlan & Craigie, 1966). Initially, it was thought Thalassiosirales (which includes *Cyclotella*) was the only diatom lineage capable of producing chitin (McLachlan & Craigie, 1966), but chitin synthases were subsequently identified in the genome of a distantly related diatom, *Phaeodactylum tricornutum* (Kroth et al., 2008). In *C. nana* (formerly *Thalassiosira pseudonana*), chitin synthases are upregulated in response to different abiotic stressors that trigger elongated cell wall morphology (Davis et al., 2005; Mock et al., 2008). Increased chitin production could strengthen the cell wall in response to increased intracellular turgor pressure. Extracellular chitin threads also promote increased buoyancy in the water column (Chiriboga & Rorrer, 2017; Morin et al., 1986). This might help diatoms optimize environmental light and temperature conditions (Boyd & Gradmann, 2002; Falciatore et al., 2000; Falciatore & Bowler, 2002), so one hypothesis is that diatoms also regulate buoyancy in response to salinity stress.

Notably, two-thirds of 21,250 thousand predicted genes in the *C. cryptica* genome have no GO annotation, and a large fraction of those were differentially expressed in at least one time point (48%) or at least two consecutive time points (12%). These latter genes in particular probably reflect important, but not yet annotated, processes that play important roles in the response to hypo-osmotic stress by diatoms. Understanding the function of uncharacterized genes is clearly a great challenge for diatom biology.

The dynamics of the transcriptional response, combined with growth analysis and comparison to long-term acclimation, allows a better understanding of how transcriptional remodelling unfolds as marine- or brackish-water diatoms acclimate to freshwater. Notably, the majority of genes with peak differential expression in the early minutes and hours following freshwater exposure returned to baseline levels within 10 h, coinciding with recovery of growth and the initial stages of freshwater acclimation. The growth rate of the newly acclimated cells was nevertheless lower than that of cells growing in the brackish control, and would probably extend for months if not in perpetuity (Nakov et al., 2020). Stress response studies in diatoms have covered a broad range of timescales (Borowitzka, 2018), with some studies focused solely on short term responses (minutes to hours) and others focused on long-term responses, in the range of days to weeks (Branco et al., 2010; Cheng et al., 2014; Krell et al., 2007, 2008; Nymark et al., 2013; Rijstenbil et al., 1989; Smith et al., 2016; Wang & Wang, 2008).

These differences in timescales have contributed to considerable debate regarding the importance of acute gene expression responses for longer term acclimation in many different experimental systems. In yeast, there is little overlap between genes differentially expressed during acute and chronic high temperatures (Shui et al., 2015), but acute expression changes are probably necessary to potentiate growth acclimation (McDaniel et al., 2018). This discrepancy

is also found in plants, where in the context of the *Arabidopsis thaliana* cold shock, only a small fraction of genes differentially expressed during acute stress play a role in long-term acclimation (Hannah et al., 2005). In contrast, the response to excess light stress in *Arabidopsis* showed a high degree of overlap for genes activated during the acute response versus those activated in long-term drought conditions associated with prolonged exposure to excess light (Crisp et al., 2017).

We found a striking lack of overlap which genes were differentially expressed during acute hypo-osmotic stress versus the months-long, acclimated response to freshwater (Nakov et al., 2020), suggesting that short-term and long-term stress acclimated responses are largely distinct. This analysis also raises questions about changes in gene expression that occur between 10 h and 120 days, highlighting the need for further studies on genomic remodelling during medium- to long-term acclimation. Nonetheless, our analyses strongly imply that the genes necessary for acute stress survival and tolerance during the early stages of growth acclimation are distinct from the genes necessary for long-term, stable growth. This study highlights how more finely resolved time courses improve our power to identify the genes important for an environmental response, while providing critical information about the processes important at different stages of acclimation.

AUTHOR CONTRIBUTIONS

Kala M. Downey, Kathryn J. Judy, Andrew J. Alverson, and Jeffrey A. Lewis conceived and designed the study. Kala M. Downey, Kathryn J. Judy conducted the experiments. Kala M. Downey, Kathryn J. Judy, and Jeffrey A. Lewis performed data analysis. Eveline Pinseel, Andrew J. Alverson, and Jeffrey A. Lewis supervised the study. Kala M. Downey wrote the original draft of the manuscript, and Eveline Pinseel, Andrew J. Alverson, and Jeffrey A. Lewis edited the manuscript. All authors have read and approve the final manuscript.

ACKNOWLEDGEMENTS

This material is based upon work supported by grants from the Simons Foundation (403249 to AJA and 725407 to EP) and the National Science Foundation (DEB-1651087 to AJA and MCB-1941824 to JAL), and multiple grants from the Arkansas Biosciences Institute (Arkansas Settlement Proceeds Act of 2000). EP also benefited from postdoctoral fellowships from Fulbright Belgium and the Belgian American Educational Foundation (BAEF). This research used resources available through the Arkansas High Performance Computing Center, which is funded through multiple NSF grants and the Arkansas Economic Development Commission. We would like to thank our reviewers for the time and effort they dedicated to providing critical and constructive reviews of this manuscript. We sincerely appreciate their valuable comments and suggestions, which helped us improve the quality of our manuscript.

CONFLICTS OF INTEREST

The authors declare no conflicts of interest.

OPEN RESEARCH BADGES

This article has eanred an Open Data badge for making publicly available the digitally-shareable data necessary to reproduce the reported results.

DATA AVAILABILITY STATEMENT

All RNA-seq data have been made available through the National Institutes of Health Gene Expression Omnibus (GEO) under accession number GSE206725. Raw and processed data plus the scripts needed to reproduce all analyses and figures are available as both Supporting Information and from Zenodo (https://doi.org/10.5281/zenodo.6704206).

ORCID

Jeffrey A. Lewis https://orcid.org/0000-0003-2952-9701

REFERENCES

Abriata, L. A., Albanesi, D., Dal Peraro, M., & de Mendoza, D. (2017). Signal sensing and transduction by histidine kinases as unveiled through studies on a temperature sensor. *Accounts of Chemical Research*, *50*(6), 1359–1366. https://doi.org/10.1021/acs.accounts.6b00593

Albert, B., Kos-Braun, I. C., Henras, A. K., Dez, C., Rueda, M. P., Zhang, X., Gadal, O., Kos, M., & Shore, D. (2019). A ribosome assembly stress response regulates transcription to maintain proteome homeostasis. *eLife*, *8*, e45002. https://doi.org/10.7554/eLife.45002

Alexa, A., & Rahnenfuhrer, J. (2022). *topGO: Enrichment analysis for gene ontology. R package version 2.48.0*.

Altschul, S. F., Gish, W., Miller, W., Myers, E. W., & Lipman, D. J. (1990). Basic local alignment search tool. *Journal of Molecular Biology*, *215*(3), 403–410. https://doi.org/10.1016/S0022-2836(05)80360-2

Anders, S., Pyl, P. T., & Huber, W. (2014). HTSeq – A Python framework to work with high-throughput sequencing data. *Bioinformatics*, *31*(2), 166–169. https://doi.org/10.1093/bioinformatics/btu638

Andrews, S. (2010). *FastQC: A quality control tool for high throughput sequence data [Online]*. http://www.bioinformatics.babraham.ac.uk/projects/fastqc/

Aramaki, T., Blanc-Mathieu, R., Endo, H., Ohkubo, K., Kanehisa, M., Goto, S., & Ogata, H. (2020). KofamKOALA: KEGG ortholog assignment based on profile HMM and adaptive score threshold. *Bioinformatics*, *36*(7), 2251–2252. https://doi.org/10.1093/bioinformatics/btz859

Balzano, S., Abs, E., & Leterme, S. C. (2015). Protist diversity along a salinity gradient in a coastal lagoon. *Aquatic Microbial Ecology*, *74*(3), 263–277. https://doi.org/10.3354/ame01740

Berry, D. B., & Gasch, A. P. (2008). Stress-activated genomic expression changes serve a preparative role for impending stress in yeast. *Molecular Biology of the Cell*, *19*(11), 4580–4587. https://doi.org/10.1091/mbc.e07-07-0680

Bilcke, G., Osuna-Cruz, C. M., Santana Silva, M., Poulsen, N., D'hondt, S., Bulankova, P., Vyverman, W., De Veylder, L., & Vandepoele, K. (2021). Diurnal transcript profiling of the diatom *Seminavis robusta* reveals adaptations to a benthic lifestyle. *The Plant Journal*, *107*(1), 315–336. https://doi.org/10.1111/tpj.15291

Booth, I. R., & Louis, P. (1999). Managing hypoosmotic stress: Aquaporins and mechanosensitive channels in *Escherichia coli*. *Current Opinion in Microbiology*, *2*(2), 166–169. https://doi.org/10.1016/S1369-5274(99)80029-0

Borowitzka, M. A. (2018). The 'stress' concept in microalgal biology—Homeostasis, acclimation and adaptation. *Journal of Applied Phycology*, *30*(5), 2815–2825. https://doi.org/10.1007/s10811-018-1399-0

Boyd, C., & Gradmann, D. (2002). Impact of osmolytes on buoyancy of marine phytoplankton. *Marine Biology*, *141*(4), 605–618. https://doi.org/10.1007/s00227-002-0872-z

Branco, D., Lima, A., Almeida, S. F. P., & Figueira, E. (2010). Sensitivity of biochemical markers to evaluate cadmium stress in the freshwater diatom *Nitzschia palea* (Kützing) W. Smith. *Aquatic Toxicology*, *99*(2), 109–117. https://doi.org/10.1016/j.aquatox.2010.04.010

Calamita, G. (2000). The *Escherichia coli* aquaporin-Z water channel. *Molecular Microbiology*, *37*(2), 254–262. https://doi.org/10.1046/j.1365-2958.2000.02016.x

Cavalcante, K. P., Tremarin, P. I., & Ludwig, T. A. V. (2013). Taxonomic studies of centric diatoms (Diatomeae): Unusual nanoplanktonic forms and new records for Brazil. *Acta Botanica Brasilica*, *27*(2), 237–251. https://doi.org/10.1590/s0102-33062013000200001

Cheng, R.-L., Feng, J., Zhang, B.-X., Huang, Y., Cheng, J., & Zhang, C.-X. (2014). Transcriptome and gene expression analysis of an oleaginous diatom under different salinity conditions. *Bioenergy Research*, *7*(1), 192–205. https://doi.org/10.1007/s12155-013-9360-1

Chiriboga, N. O. G., & Rorrer, G. L. (2017). Control of chitin nanofiber production by the lipid-producing diatom *Cyclotella* sp. through fed-batch addition of dissolved silicon and nitrate in a bubble-column photobioreactor. *Biotechnology Progress*, *33*(2), 407–415. https://doi.org/10.1002/btpr.2445

Conley, D. J., Kilham, S. S., & Theriot, E. (1989). Differences in silica content between marine and freshwater diatoms. *Limnology and Oceanography*, *34*(1), 205–212. https://doi.org/10.4319/lo.1989.34.1.0205

Crisp, P. A., Ganguly, D. R., Smith, A. B., Murray, K. D., Estavillo, G. M., Searle, I., Ford, E., Bogdanović, O., Lister, R., Borevitz, J. O., Eichten, S. R., & Pogson, B. J. (2017). Rapid recovery gene downregulation during excess-light stress and recovery in *Arabidopsis*. *The Plant Cell*, *29*(8), 1836–1863. https://doi.org/10.1105/tpc.16.00828

Davies, K. J. A. (2016). Adaptive homeostasis. *Molecular Aspects of Medicine*, *49*, 1–7. https://doi.org/10.1016/j.mam.2016.04.007

Davis, A. K., Hildebrand, M., & Palenik, B. (2005). A stress-induced protein associated with the girdle band region of the diatom *Thalassiosira pseudonana* (bacillariophyta). *Journal of Phycology*, *41*(3), 577–589. https://doi.org/10.1111/j.1529-8817.2005.00076.x

Dickson, D. M. J., & Kirst, G. O. (1987). Osmotic adjustment in marine eukaryotic algae: The role of inorganic ions, quaternary ammonium, tertiary sulphonium and carbohydrate solutes. *New Phytologist*, *106*(4), 645–655. https://doi.org/10.1111/j.1469-8137.1987.tb00165.x

Dobin, A., & Gingeras, T. R. (2015). Mapping RNA-seq reads with STAR. *Current Protocols in Bioinformatics*, *51*, 11.14.11–11.14.19. https://doi.org/10.1002/0471250953.bi1114s51

Durkin, C. A., Mock, T., & Armbrust, E. V. (2009). Chitin in diatoms and its association with the cell wall. *Eukaryotic Cell*, *8*(7), 1038–1050. https://doi.org/10.1128/EC.00079-09

Eisen, M. B., Spellman, P. T., Brown, P. O., & Botstein, D. (1998). Cluster analysis and display of genome-wide expression patterns. *Proceedings of the National Academy of Sciences of the United States of America*, *95*(25), 14863–14868. https://doi.org/10.1073/pnas.95.25.14863

Emms, D. M., & Kelly, S. (2015). OrthoFinder: Solving fundamental biases in whole genome comparisons dramatically improves orthogroup inference accuracy. *Genome Biology*, *16*(1), 157. https://doi.org/10.1186/s13059-015-0721-2

Evans, D. H. (2009). *Osmotic and ionic regulation: Cells and animals*. CRC Press.

Falciatore, A., & Bowler, C. (2002). Revealing the molecular secrets of marine diatoms. *Annual Review of Plant Biology*, *53*, 109–130. https://doi.org/10.1146/annurev.arplant.53.091701.153921

Falciatore, A., d'Alcalà, M. R., Croot, P., & Bowler, C. (2000). Perception of environmental signals by a marine diatom. *Science*, *288*(5475), 2363–2366. https://doi.org/10.1126/science.288.5475.2363

Gasch, A. P., Spellman, P. T., Kao, C. M., Carmel-Harel, O., Eisen, M. B., Storz, G., Botstein, D., & Brown, P. O. (2000). Genomic expression programs in the response of yeast cells to environmental changes. *Molecular Biology of the Cell*, *11*(12), 4241–4257. https://doi.org/10.1091/mbc.11.12.4241

Godhe, A., Kremp, A., & Montresor, M. (2014). Genetic and microscopic evidence for sexual reproduction in the centric diatom *Skeletonema marinoi*. *Protist*, *165*(4), 401–416. https://doi.org/10.1016/j.protis.2014.04.006

Goldman, J. A. L., Schatz, M. J., Berthiaume, C. T., Coesel, S. N., Orellana, M. V., & Armbrust, E. V. (2019). Fe limitation decreases transcriptional regulation over the diel cycle in the model diatom *Thalassiosira pseudonana*. *PLoS One*, *14*(9), e0222325. https://doi.org/10.1371/journal.pone.0222325

Ha, H. C., Yager, J. D., Woster, P. A., & Casero, R. A. (1998). Structural specificity of polyamines and polyamine analogues in the protection of DNA from strand breaks induced by reactive oxygen species. *Biochemical and Biophysical Research Communications*, *244*(1), 298–303. https://doi.org/10.1006/bbrc.1998.8258

Hannah, M. A., Heyer, A. G., & Hincha, D. K. (2005). A global survey of gene regulation during cold acclimation in *Arabidopsis thaliana*. *PLoS Genetics*, *1*(2), e26. https://doi.org/10.1371/journal.pgen.0010026

Hayat, S., Hayat, Q., Alyemeni, M. N., Wani, A. S., Pichtel, J., & Ahmad, A. (2012). Role of proline under changing environments. *Plant Signaling & Behavior*, *7*(11), 1456–1466. https://doi.org/10.4161/psb.21949

Heller, R., Manduchi, E., Grant, G. R., & Ewens, W. J. (2009). A flexible two-stage procedure for identifying gene sets that are differentially expressed. *Bioinformatics*, *25*(8), 1019–1025. https://doi.org/10.1093/bioinformatics/btp076

Ho, Y.-H., Shishkova, E., Hose, J., Coon, J. J., & Gasch, A. P. (2018). Decoupling yeast cell division and stress defense implicates mRNA repression in translational reallocation during stress. *Current Biology*, *28*(16), 2673–2680.e2674. https://doi.org/10.1016/j.cub.2018.06.044

Hohmann, S. (2002). Osmotic stress signaling and osmoadaptation in yeasts. *Microbiology and Molecular Biology Reviews*, *66*(2), 300–372. https://doi.org/10.1128/mmbr.66.2.300-372.2002

Houk, V., Klee, R., & Tanaka, H. (2010). Atlas of freshwater centric diatoms with a brief key and descriptions Part III. Stephanodiscaceae A *Cyclotella*, *Tertiarius*, *Discostella*. *Fottea*, *10*, 1–498.

Jahn, T. P., Møller, A. L. B., Zeuthen, T., Holm, L. M., Klaerke, D. A., Mohsin, B., Kühlbrandt, W., & Schjoerring, J. K. (2004). Aquaporin homologues in plants and mammals transport ammonia. *FEBS Letters*, *574*(1–3), 31–36. https://doi.org/10.1016/j.febslet.2004.08.004

Kageyama, H., Tanaka, Y., & Takabe, T. (2018). Biosynthetic pathways of glycinebetaine in *Thalassiosira pseudonana*; functional characterization of enzyme catalyzing three-step methylation of glycine. *Plant Physiology and Biochemistry*, *127*, 248–255. https://doi.org/10.1016/j.plaphy.2018.03.032

Kirst, G. O. (1990). Salinity tolerance of eukaryotic marine algae. *Annual Review of Plant Physiology and Plant Molecular Biology*, *41*(1), 21–53. https://doi.org/10.1146/annurev.pp.41.060190.000321

Krell, A., Beszteri, B., Dieckmann, G., Glöckner, G., Valentin, K., & Mock, T. (2008). A new class of ice-binding proteins discovered in a salt-stress-induced cDNA library of the psychrophilic diatom *Fragilariopsis cylindrus* (Bacillariophyceae). *European Journal of Phycology*, *43*(4), 423–433. https://doi.org/10.1080/09670260802348615

Krell, A., Funck, D., Plettner, I., John, U., & Dieckmann, G. (2007). Regulation of proline metabolism under salt stress in the psychrophilic diatom *Fragilariopsis cylindrus* (Bacillariophyceae). *Journal of Phycology*, *43*(4), 753–762. https://doi.org/10.1111/j.1529-8817.2007.00366.x

Kroth, P. G., Chiovitti, A., Gruber, A., Martin-Jezequel, V., Mock, T., Parker, M. S., Stanley, M. S., Kaplan, A., Caron, L., Weber, T., Maheswari,

U., Armbrust, E. V., & Bowler, C. (2008). A model for carbohydrate metabolism in the diatom *Phaeodactylum tricornutum* deduced from comparative whole genome analysis. *PLoS One*, *3*(1), e1426. https://doi.org/10.1371/journal.pone.0001426

Kültz, D., Podrabsky, J. E., Stillman, J. H., & Tomanek, L. (2015). Physiological mechanisms used by fish to cope with salinity stress. *Journal of Experimental Biology*, *218*(12), 1907–1914. https://doi.org/10.1242/jeb.118695

Kung, C., Martinac, B., & Sukharev, S. (2010). Mechanosensitive channels in microbes. *Annual Review of Microbiology*, *64*, 313–329. https://doi.org/10.1146/annurev.micro.112408.134106

Kunz, H.-H., Gierth, M., Herdean, A., Satoh-Cruz, M., Kramer, D. M., Spetea, C., & Schroeder, J. I. (2014). Plastidial transporters KEA1, -2, and -3 are essential for chloroplast osmoregulation, integrity, and pH regulation in *Arabidopsis*. *Proceedings of the National Academy of Sciences of the United States of America*, *111*(20), 7480–7485. https://doi.org/10.1073/pnas.1323899111

Latowski, D., Kuczyńska, P., & Strzałka, K. (2011). Xanthophyll cycle – A mechanism protecting plants against oxidative stress. *Redox Report*, *16*(2), 78–90. https://doi.org/10.1179/174329211x13020951739938

LeDuff, P., & Rorrer, G. L. (2019). Formation of extracellular β-chitin nanofibers during batch cultivation of marine diatom *Cyclotella* sp. at silicon limitation. *Journal of Applied Phycology*, *31*(6), 3479–3490. https://doi.org/10.1007/s10811-019-01879-6

Lee, C. E., Downey, K., Colby, R. S., Freire, C. A., Nichols, S., Burgess, M. N., & Judy, K. J. (2022). Recognizing salinity threats in the climate crisis. *Integrative and Comparative Biology*, *62*, 441–460. https://doi.org/10.1093/icb/icac069

Lee, M. V., Topper, S. E., Hubler, S. L., Hose, J., Wenger, C. D., Coon, J. J., & Gasch, A. P. (2011). A dynamic model of proteome changes reveals new roles for transcript alteration in yeast. *Molecular Systems Biology*, *7*, 514. https://doi.org/10.1038/msb.2011.48

Liang, Y., Zhang, M., Wang, M., Zhang, W., Qiao, C., Luo, Q., Lu, X., & Kelly, R. M. (2020). Freshwater cyanobacterium *Synechococcus elongatus* PCC 7942 adapts to an environment with salt stress via ion-induced enzymatic balance of compatible solutes. *Applied and Environmental Microbiology*, *86*(7), e02904-19. https://doi.org/10.1128/aem.02904-19

Liu, M. S., & Hellebust, J. A. (1974). Uptake of amino acids by the marine centric diatom *Cyclotella cryptica*. *Canadian Journal of Botany*, *20*(8), 1109–1118. https://doi.org/10.1139/m74-173

Liu, M. S., & Hellebust, J. A. (1976). Effects of salinity and osmolarity of the medium on amino acid metabolism in *Cyclotella cryptica*. *Canadian Journal of Microbiology*, *54*(9), 938–948. https://doi.org/10.1139/b76-098

Lund, S. P., Nettleton, D., McCarthy, D. J., & Smyth, G. K. (2012). Detecting differential expression in RNA-sequence data using quasi-likelihood with shrunken dispersion estimates. *Statistical Applications in Genetics and Molecular Biology*, *11*(5). https://doi.org/10.1515/1544-6115.1826

Lyon, B. R., Bennett-Mintz, J. M., Lee, P. A., Janech, M. G., & DiTullio, G. R. (2016). Role of dimethylsulfoniopropionate as an osmoprotectant following gradual salinity shifts in the sea-ice diatom *Fragilariopsis cylindrus*. *Environmental Chemistry*, *13*(2), 181–194. https://doi.org/10.1071/EN14269

Lyon, B. R., Lee, P. A., Bennett, J. M., DiTullio, G. R., & Janech, M. G. (2011). Proteomic analysis of a sea-ice diatom: Salinity acclimation provides new insight into the dimethylsulfoniopropionate production pathway. *Plant Physiology*, *157*(4), 1926–1941. https://doi.org/10.1104/pp.111.185025

Mager, W. H., & De Kruijff, A. J. (1995). Stress-induced transcriptional activation. *Microbiology Reviews*, *59*(3), 506–531. https://doi.org/10.1128/mr.59.3.506-531.1995

Matsui, H., Hopkinson, B., Nakajima, K., & Matsuda, Y. (2018). Plasma-membrane-type aquaporins from marine diatoms function as CO_2/NH_3 channels and provide photoprotection. *Plant Physiology*, *178*(1), 345–357. https://doi.org/10.1104/pp.18.00453

Mayer, C., Bierhoff, H., & Grummt, I. (2005). The nucleolus as a stress sensor: JNK2 inactivates the transcription factor TIF-IA and down-regulates rRNA synthesis. *Genes & Development*, *19*(8), 933–941. https://doi.org/10.1101/gad.333205

McDaniel, E. A., Stuecker, T. N., Veluvolu, M., Gasch, A. P., & Lewis, J. A. (2018). Independent mechanisms for acquired salt tolerance versus growth resumption induced by mild ethanol pretreatment in *Saccharomyces cerevisiae*. *mSphere*, *3*(6), e00574-18. https://doi.org/10.1128/mSphere.00574-18

McLachlan, J., & Craigie, J. S. (1966). Chitan fibres in *Cyclotella cryptica* and growth of *C. cryptica* and *Thalassiosira fluviatilis*. In H. Barnes (Ed.), *Some contemporary studies in marine science* (pp. 511–517). George Allen and Unwin Ltd.

Mock, T., Samanta, M. P., Iverson, V., Berthiaume, C., Robison, M., Holtermann, K., Durkin, C., BonDurant, S. S., Richmond, K., Rodesch, M., Kallas, T., Huttlin, E. L., Cerrina, F., Sussman, M. R., & Armbrust, E. V. (2008). Whole-genome expression profiling of the marine diatom *Thalassiosira pseudonana* identifies genes involved in silicon bioprocesses. *Proceedings of the National Academy of Sciences of the United States of America*, *105*(5), 1579–1584. https://doi.org/10.1073/pnas.0707946105

Morin, L. G., Smucker, R. A., & Herth, W. (1986). Effects of two chitin synthesis inhibitors on *Thalassiosira fluviatilis* and *Cyclotella cryptica*. *FEMS Microbiology Letters*, *37*(3), 263–268. https://doi.org/10.1111/j.1574-6968.1986.tb01806.x

Nakov, T., Beaulieu, J. M., & Alverson, A. J. (2018). Insights into global planktonic diatom diversity: The importance of comparisons between phylogenetically equivalent units that account for time. *The ISME Journal*, *12*(11), 2807–2810. https://doi.org/10.1038/s41396-018-0221-y

Nakov, T., Judy, K. J., Downey, K. M., Ruck, E. C., & Alverson, A. J. (2020). Transcriptional response of osmolyte synthetic pathways and membrane transporters in a euryhaline diatom during long-term acclimation to a salinity gradient. *Journal of Phycology*, *56*, 1712–1728.

Negrão, S., Schmöckel, S. M., & Tester, M. (2017). Evaluating physiological responses of plants to salinity stress. *Annals of Botany*, *119*(1), 1–11. https://doi.org/10.1093/aob/mcw191

Nitta, M., Okamura, H., Aizawa, S., & Yamaizumi, M. (1997). Heat shock induces transient p53-dependent cell cycle arrest at G1/S. *Oncogene*, *15*(5), 561–568. https://doi.org/10.1038/sj.onc.1201210

Nymark, M., Valle, K. C., Hancke, K., Winge, P., Andresen, K., Johnsen, G., Bones, A. M., & Brembu, T. (2013). Molecular and photosynthetic responses to prolonged darkness and subsequent acclimation to re-illumination in the diatom *Phaeodactylum tricornutum*. *PLoS One*, *8*(3), e58722. https://doi.org/10.1371/journal.pone.0058722

Papenbrock, J., Mock, H. P., Tanaka, R., Kruse, E., & Grimm, B. (2000). Role of magnesium chelatase activity in the early steps of the tetrapyrrole biosynthetic pathway. *Plant Physiology*, *122*(4), 1161–1169. https://doi.org/10.1104/pp.122.4.1161

Pinseel, E., Nakov, T., Van den Berge, K., Downey, K. M., Judy, K. J., Kourtchenko, O., Kremp, A., Ruck, E. C., Sjöqvist, C., Töpel, M., Godhe, A., & Alverson, A. J. (2022). Strain-specific transcriptional responses overshadow salinity effects in a marine diatom sampled along the Baltic Sea salinity cline. *The ISME Journal*, *16*(7), 1776–1787. https://doi.org/10.1038/s41396-022-01230-x

Pörtner, H.-O., Roberts, D. C., Masson-Delmotte, V., Zhai, P., Tignor, M., Poloczanska, E., & Weyer, N. M. (2019). The ocean and cryosphere in a changing climate. In *IPCC special report on the ocean and cryosphere in a changing climate* (pp. 447–588).

Rangel, D. E. N. (2011). Stress induced cross-protection against environmental challenges on prokaryotic and eukaryotic microbes. *World Journal of Microbiology and Biotechnology*, *27*(6), 1281–1296. https://doi.org/10.1007/s11274-010-0584-3

Reimann, B. E. F., Lewin, J. M. C., & Guillard, R. R. L. (1963). *Cyclotella cryptica*, a new brackish-water diatom species. *Phycologia*, *3*(2), 75–84. https://doi.org/10.2216/i0031-8884-3-2-75.1

Rijstenbil, J. W., Wijnholds, J. A., & Sinke, J. J. (1989). Implications of salinity fluctuation for growth and nitrogen metabolism of the marine diatom *Ditylum brightwellii* in comparison with *Skeletonema costatum*. *Marine Biology*, *101*(1), 131–141. https://doi.org/10.1007/BF00393486

Ritchie, M. E., Phipson, B., Wu, D., Hu, Y., Law, C. W., Shi, W., & Smyth, G. K. (2015). limma powers differential expression analyses for RNA-sequencing and microarray studies. *Nucleic Acids Research*, *43*(7), e47. https://doi.org/10.1093/nar/gkv007

Roberts, W. R., Downey, K. M., Ruck, E. C., Traller, J. C., & Alverson, A. J. (2020). Improved reference genome for *Cyclotella cryptica* CCMP332, a model for cell wall morphogenesis, salinity adaptation, and lipid production in diatoms (Bacillariophyta). *G3 Genes|Genomes|Genetics*, *10*(9), 2965–2974. https://doi.org/10.1534/g3.120.401408

Roberts, W. R., Ruck, E. C., Downey, K. M., & Alverson, A. J. (2022). Resolving marine–freshwater transitions by diatoms through a fog of gene tree discordance and hemiplasy. *bioRxiv*. https://doi.org/10.1101/2022.08.12.503770

Robinson, M. D., McCarthy, D. J., & Smyth, G. K. (2010). edgeR: A Bioconductor package for differential expression analysis of digital gene expression data. *Bioinformatics*, *26*(1), 139–140. https://doi.org/10.1093/bioinformatics/btp616

Rojas, E. R., Huang, K. C., & Theriot, J. A. (2017). Homeostatic cell growth is accomplished mechanically through membrane tension inhibition of cell-wall synthesis. *Cell Systems*, *5*(6), 578–590. https://doi.org/10.1016/j.cels.2017.11.005

Sabehat, A., Weiss, D., & Lurie, S. (1998). Heat-shock proteins and cross-tolerance in plants. *Physiologia Plantarum*, *103*(3), 437–441. https://doi.org/10.1034/j.1399-3054.1998.1030317.x

Schulte, P. M. (2014). What is environmental stress? Insights from fish living in a variable environment. *Journal of Experimental Biology*, *217*(1), 23–34. https://doi.org/10.1242/jeb.089722

Schultz, E. T., & McCormick, S. D. (2012). Euryhalinity in an evolutionary context. In S. D. McCormick, A. P. Farrell, & C. J. Brauner (Eds.), *Euryhaline fishes* (pp. 477–533). Academic Press.

Schultz, M. E. (1971). Salinity-related polymorphism in the brackish-water diatom *Cyclotella cryptica*. *Canadian Journal of Botany*, *49*(8), 1285–1289. https://doi.org/10.1139/b71-182

Schultz, M. E., & Trainor, F. R. (1970). Production of male gametes and auxospores in a polymorphic clone of the centric diatom *Cyclotella*. *Canadian Journal of Botany*, *48*(5), 947–951. https://doi.org/10.1139/b70-133

Seaton, D. D., & Krishnan, J. (2016). Model-based analysis of cell cycle responses to dynamically changing environments. *PLoS Computational Biology*, *12*(1), e1004604. https://doi.org/10.1371/journal.pcbi.1004604

Sharfstein, S. T., Shen, D., Kiehl, T. R., & Zhou, R. (2007). Molecular response to osmotic shock. In M. Al-Rubeai, & M. Fussenegger (Eds.), *Systems biology* (pp. 213–236). Springer.

Sheng, P., Tan, J., Jin, M., Wu, F., Zhou, K., Ma, W., Heng, Y., Wang, J., Guo, X., Zhang, X., Cheng, Z., Liu, L., Wang, C., Liu, X., & Wan, J. (2014). *Albino midrib 1*, encoding a putative potassium efflux antiporter, affects chloroplast development and drought tolerance in rice. *Plant Cell Reports*, *33*(9), 1581–1594. https://doi.org/10.1007/s00299-014-1639-y

Shu, Q., Qiao, F., Song, Z., Zhao, J., & Li, X. (2018). Projected freshening of the arctic ocean in the 21st century. *Journal of Geophysical Research, C: Oceans*, *123*(12), 9232–9244. https://doi.org/10.1029/2018jc014036

Shui, W., Xiong, Y., Xiao, W., Qi, X., Zhang, Y., Lin, Y., Guo, Y., Zhang, Z., Wang, Q., & Ma, Y. (2015). Understanding the Mechanism of thermotolerance distinct from heat shock response through proteomic analysis of industrial strains of saccharomyces cerevisiae. *Molecular & Cellular Proteomics*, *14*(7), 1885–1897. https://doi.org/10.1074/mcp.m114.045781

Skirycz, A., Claeys, H., De Bodt, S., Oikawa, A., Shinoda, S., Andriankaja, M., Maleux, K., Eloy, N. B., Coppens, F., Yoo, S.-D., Saito, K., & Inzé, D. (2011). Pause-and-stop: The effects of osmotic stress on cell proliferation during early leaf development in *Arabidopsis* and a role for ethylene signaling in cell cycle arrest. *The Plant Cell*, *23*(5), 1876–1888. https://doi.org/10.1105/tpc.111.084160

Smith, S. R., Gillard, J. T. F., Kustka, A. B., McCrow, J. P., Badger, J. H., Zheng, H., Ashley, M. N., Dupont, C. L., Obata, T., Fernie, A. R., & Allen, A. E. (2016). Transcriptional orchestration of the global cellular response of a model pennate diatom to diel light cycling under iron limitation. *PLoS Genetics*, *12*(12), e1006490. https://doi.org/10.1371/journal.pgen.1006490

Storey, A. J., Hardman, R. E., Byrum, S. D., Mackintosh, S. G., Edmondson, R. D., Wahls, W. P., Tackett, A. J., & Lewis, J. A. (2020). Accurate and sensitive quantitation of the dynamic heat shock proteome using tandem mass tags. *Journal of Proteome Research*, *19*(3), 1183–1195. https://doi.org/10.1021/acs.jproteome.9b00704

Sun, K. (2020). Ktrim: An extra-fast and accurate adapter- and quality-trimmer for sequencing data. *Bioinformatics*, *36*(11), 3561–3562. https://doi.org/10.1093/bioinformatics/btaa171

Supek, F., Bošnjak, M., Škunca, N., & Šmuc, T. (2011). REVIGO summarizes and visualizes long lists of gene ontology terms. *PLoS One*, *6*(7), e21800. https://doi.org/10.1371/journal.pone.0021800

Tanghe, A., Van Dijck, P., & Thevelein, J. M. (2006). Why do microorganisms have aquaporins? *Trends in Microbiology*, *14*(2), 78–85. https://doi.org/10.1016/j.tim.2005.12.001

Tevatia, R., Allen, J., Rudrappa, D., White, D., Clemente, T. E., Cerutti, H., Demirel, Y., & Blum, P. (2015). The taurine biosynthetic pathway of microalgae. *Algal Research*, *9*, 21–26. https://doi.org/10.1016/j.algal.2015.02.012

Theseira, A. M., Nielsen, D. A., & Petrou, K. (2020). Uptake of dimethylsulphoniopropionate (DMSP) reduces free reactive oxygen species (ROS) during late exponential growth in the diatom *Thalassiosira weissflogii* grown under three salinities. *Marine Biology*, *167*(9). 1–7. https://doi.org/10.1007/s00227-020-03744-4

Traller, J. C., Cokus, S. J., Lopez, D. A., Gaidarenko, O., Smith, S. R., McCrow, J. P., Gallaher, S. D., Podell, S., Thompson, M., Cook, O., Morselli, M., Jaroszewicz, A., Allen, E. E., Allen, A. E., Merchant, S. S., Pellegrini, M., & Hildebrand, M. (2016). Genome and methylome of the oleaginous diatom *Cyclotella cryptica* reveal genetic flexibility toward a high lipid phenotype. *Biotechnology for Biofuels and Bioproducts*, *9*, 258. https://doi.org/10.1186/s13068-016-0670-3

Tyerman, S. D., McGaughey, S. A., Qiu, J., Yool, A. J., & Byrt, C. S. (2021). Adaptable and multifunctional ion-conducting aquaporins. *Annual Review of Plant Biology*, *72*, 703–736. https://doi.org/10.1146/annurev-arplant-081720-013608

Tyerman, S. D., Niemietz, C. M., & Bramley, H. (2002). Plant aquaporins: Multifunctional water and solute channels with expanding roles. *Plant, Cell & Environment*, *25*(2), 173–194. https://doi.org/10.1046/j.0016-8025.2001.00791.x

Van Bergeijk, S. A., Van der Zee, C., & Stal, L. J. (2003). Uptake and excretion of dimethylsulphoniopropionate is driven by salinity changes in the marine benthic diatom *Cylindrotheca closterium*. *European Journal of Phycology*, *38*(4), 341–349. https://doi.org/10.1080/0967026031000161260

Van den Berge, K., Soneson, C., Robinson, M. D., & Clement, L. (2017). stageR: A general stage-wise method for controlling the gene-level false discovery rate in differential expression and differential transcript usage. *Genome Biology*, *18*(1), 151. https://doi.org/10.1186/s13059-017-1277-0

Wang, M.-J., & Wang, W.-X. (2008). Temperature-dependent sensitivity of a marine diatom to cadmium stress explained by subcelluar

distribution and thiol synthesis. *Environmental Science & Technology*, *42*(22), 8603–8608. https://doi.org/10.1021/es801470w

Warner, J. R. (1999). The economics of ribosome biosynthesis in yeast. *Trends in Biochemical Sciences*, *24*(11), 437–440. https://doi.org/10.1016/s0968-0004(99)01460-7

West, G., Inzé, D., & Beemster, G. T. S. (2004). Cell cycle modulation in the response of the primary root of *Arabidopsis* to salt stress. *Plant Physiology*, *135*(2), 1050–1058. https://doi.org/10.1104/pp.104.040022

Zanotto, F. P., & Wheatly, M. G. (2006). Ion regulation in invertebrates: Molecular and integrative aspects. *Physiological and Biochemical Zoology*, *79*(2), 357–362. https://doi.org/10.1086/499993

Zhu, J.-K. (2001). Cell signaling under salt, water and cold stresses. *Current Opinion in Plant Biology*, *4*(5), 401–406. https://doi.org/10.1016/s1369-5266(00)00192-8

SUPPORTING INFORMATION

Additional supporting information can be found online in the Supporting Information section at the end of this article.

How to cite this article: Downey, K. M., Judy, K. J., Pinseel, E., Alverson, A. J., & Lewis, J. A. (2023). The dynamic response to hypo-osmotic stress reveals distinct stages of freshwater acclimation by a euryhaline diatom. *Molecular Ecology*, *32*, 2766–2783. https://doi.org/10.1111/mec.16703